

# **REPORT 1233**

---

## **SHOCK-TURBULENCE INTERACTION AND THE GENERATION OF NOISE**

**By H. S. RIBNER**

**Lewis Flight Propulsion Laboratory  
Cleveland, Ohio**

**Ad-A 278325**

**Best Available Copy**

**DTIC QUALITY INSPECTED 3**

# National Advisory Committee for Aeronautics

*Headquarters, 1512 H Street NW., Washington 25, D. C.*

Created by act of Congress approved March 3, 1915, for the supervision and direction of the scientific study of the problems of flight (U. S. Code, title 50, sec. 151). Its membership was increased from 12 to 15 by act approved March 2, 1929, and to 17 by act approved May 25, 1948. The members are appointed by the President, and serve as such without compensation.

JEROME C. HUNSAKER, Sc. D., Massachusetts Institute of Technology, *Chairman*

LEONARD CARMICHAEL, Ph. D., Secretary, Smithsonian Institution, *Vice Chairman*

JOSEPH P. ADAMS, LL. B., Vice Chairman, Civil Aeronautics Board.  
ALLEN V. ASTIN, Ph. D., Director, National Bureau of Standards.  
PRESTON R. BASSETT, M. A., Vice President, Sperry Rand Corp.  
DETLEV W. BRONK, Ph. D., President, Rockefeller Institute for Medical Research.  
THOMAS S. COMBS, Vice Admiral, United States Navy, Deputy Chief of Naval Operations (Air).  
FREDERICK C. CRAWFORD, Sc. D., Chairman of the Board, Thompson Products, Inc.  
RALPH S. DAMON, D. Eng., President, Trans World Airlines, Inc.  
JAMES H. DOOLITTLE, Sc. D., Vice President, Shell Oil Co.  
CARL J. PFINGSTAG, Rear Admiral, United States Navy, Assistant Chief for Field Activities, Bureau of Aeronautics.

DONALD L. PUTT, Lieutenant General, United States Air Force, Deputy Chief of Staff (Development).  
DONALD A. QUARLES, D. Eng., Secretary of the Air Force.  
ARTHUR E. RAYMOND, Sc. D., Vice President Engineering, Douglas Aircraft Co., Inc.  
FRANCIS W. REICHELDERFER, Sc. D., Chief, United States Weather Bureau.  
LOUIS S. ROTHSCHILD, Ph. B., Under Secretary of Commerce for Transportation.  
NATHAN F. TWINING, General, United States Air Force, Chief of Staff.

---

HUGH L. DRYDEN, Ph. D., *Director*

JOHN F. VICTORY, LL. D., *Executive Secretary*

JOHN W. CROWLEY, JR., B. S., *Associate Director for Research*

EDWARD H. CHAMBERLIN, *Executive Officer*

---

HENRY J. E. REID, D. Eng., Director, Langley Aeronautical Laboratory, Langley Field, Va.

SMITH J. DEFANCE, D. Eng., Director, Ames Aeronautical Laboratory, Moffett Field, Calif.

EDWARD R. SHARP, Sc. D., Director, Lewis Flight Propulsion Laboratory, Cleveland, Ohio

WALTER C. WILLIAMS, B. S., Chief, High-Speed Flight Station, Edwards, Calif.

# CONTENTS

	Page
SUMMARY	1
INTRODUCTION	1
SHOCK INTERACTION OF SINGLE SHEAR WAVE	1
Qualitative Discussion	1
Quantitative Discussion	2
Elementary wave	2
Geometric reexamination of prior results	3
Initial shear wave ( $\sim$ initial turbulence)	3
Refracted shear-entropy wave ( $\sim$ final turbulence and entropy spottiness)	3
Generated sound wave ( $\sim$ noise field)	4
Transformation to Cartesian coordinates	4
SPECTRAL ANALYSIS OF RANDOM FIELDS	4
Homogeneous Fields	5
Amplitude spectra	5
Correlations	5
Correlation and power spectra	5
Correlation spectrum in terms of amplitude spectra	5
Inhomogeneous Fields	6
Correlation of Two-Dimensional Field with Three-Dimensional Field	6
SHOCK INTERACTION OF SPECTRUM OF SHEAR WAVES (TURBULENCE)	7
Diagonal Terms of Velocity Spectrum Tensor	7
Turbulence field	7
Noise field	7
Mean-Square Velocity Components	7
Turbulence field	7
Noise field	7
Mean-Square Pressure	8
Mean-Square Temperature	8
Mean-Square Density	8
Correlations Not Jointly Involving Turbulence and Noise	8
Attempts at simplification	8
Cross-correlations	9
Correlations Between Turbulence and Noise	9
Interaction of Turbulence with an Oblique Shock	10
CALCULATIONS	10
Mean-Square Velocity Components in Turbulence Field	10
Mean-Square Temperature in Entropy Field	11
Mean-Square Pressure in Noise Field	11
RESULTS AND DISCUSSION	11
CONCLUDING REMARKS	13
APPENDIXES	13
A. SYMBOLS	13
B. COMPLETE VELOCITY SPECTRUM TENSORS	14
Turbulence field	14
Noise field	15
C. CALCULATIONS FOR AXISYMMETRIC INITIAL TURBULENCE	15
REFERENCES	16
TABLE	17

Accession For	
NTIS GRA&I	<input checked="" type="checkbox"/>
DTIC TAB	<input type="checkbox"/>
Unannounced	<input type="checkbox"/>
Justification	
By	
Distribution/	
Availability Codes	
Dist	Avail and/or Special
A-1	

## REPORT 1233

# SHOCK-TURBULENCE INTERACTION AND THE GENERATION OF NOISE<sup>1</sup>

By H. S. RIBNER

### SUMMARY

*The interaction of a convected field of turbulence with a shock wave has been analyzed to yield the modified turbulence, entropy spottiness, and noise generated downstream of the shock. This analysis generalizes the results of Technical Report 1164, which apply to a single spectrum component, to give the shock-interaction effects of a complete turbulence field. The previous report solved the basic gas-dynamic problem, and the present report has added the necessary spectrum analysis.*

*Formulas for spectra and correlations have been obtained and numerical calculations have been carried out to yield curves of root-mean-square velocity components, temperature, pressure, and noise in decibels against Mach number for the Mach number range of 1 to  $\infty$ ; both isotropic and strongly axisymmetric (lateral perturbations/longitudinal perturbations  $\approx 36/1$ ) initial turbulence have been treated. It was found that in either case initial turbulence with a longitudinal component of 0.1 percent of stream velocity would yield a noise pressure level of about 120 decibels; the value of lateral component had relatively little effect.*

*The present results are applicable quantitatively to flow in ducts or channels containing normal shocks; they are presumed to provide a qualitative guide to the generation of noise by the shock structure in a supersonic free jet.*

### INTRODUCTION

The propulsion of aircraft by means of jets gives rise to intense noise as an unfortunate byproduct. Programs of noise abatement are under way, but at present they are largely empirical: even with the general guide provided by Lighthill's theory (ref. 1), the understanding of the mechanisms of noise generation is far from complete. It appears from both experimental and theoretical evidence, however, that the interaction of turbulence with shock waves must often play a part. On the theoretical side, the generation of noise by such interaction is pointed out independently in references 2 and 3. The shock-turbulence interaction was found to produce, in addition to the noise, an entropy "spottiness" aft of the shock (manifested as a temperature and density spottiness at constant pressure, ref. 2).

Turbulence, entropy spottiness, and noise (pressure fluctuations) are examples of the three fundamental modes of small disturbance perturbation of a gas (refs. 4 and 5); more specifically, the categories are vorticity mode, entropy mode, and sound mode. The vorticity mode (turbulence)

and the entropy mode are essentially "frozen" patterns (to use Kovásznyai's term) that are convected by the main flow; the sound mode, however, consists of waves that propagate in various directions in addition to being convected.

To the first order in the perturbation velocity, there is no tendency for the modes to interact or for an isolated mode to spontaneously generate one of the other modes (ref. 5). (The weak transference of turbulence into noise described by the Lighthill theory is a higher-order effect (ref. 1).) The presence of a shock wave, however, provides a mechanism for a very strong transference: thus, when any one of the three modes—turbulence, entropy spottiness, or noise—encounters a shock, the interaction will give rise to all three modes, in comparable strength, downstream of the shock (refs. 2, 4, and 6).

The first of these cases, shock-turbulence interaction, has been investigated at the NACA Lewis laboratory as an outgrowth of reference 2 and is reported herein. The analysis of the earlier paper was concerned with a single spectrum wave of a turbulent field and was primarily a study in gas dynamics. The present paper reformulates the results and incorporates them in a spectral analysis; from the analysis come the quantitative effects of the interaction of a convected homogeneous field of turbulence with an extended plane shock front. (Some results of this work are reported in abbreviated form in refs. 7 and 8.) The perturbation velocity, pressure, temperature, and density distributions behind the shock are described in terms of formulas for their spectra, correlations, and mean-square values; these are separated into the respective contributions of turbulence, entropy spottiness, and noise.

Numerical calculations are presented for the root-mean-square values of the pressure (noise) and components of the temperature and velocity perturbations for the Mach number range of 1 to  $\infty$ ; one set of calculations refers to isotropic initial turbulence, another set to strongly axisymmetric initial turbulence (lateral perturbations/longitudinal perturbations  $\approx 36/1$ ). The noise pressure level is also presented on an acoustic scale for several levels of initial turbulence.

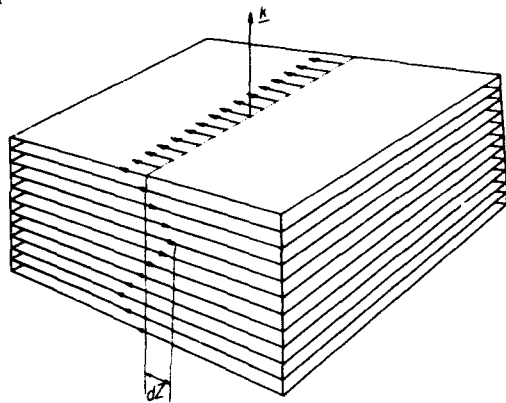
### SHOCK INTERACTION OF SINGLE SHEAR WAVE

#### QUALITATIVE DISCUSSION

According to the Fourier integral theorem, a turbulent velocity field can be represented as a superposition or spectrum of elementary waves. A single spectrum wave can be interpreted physically as a plane sinusoidal wave of shear-

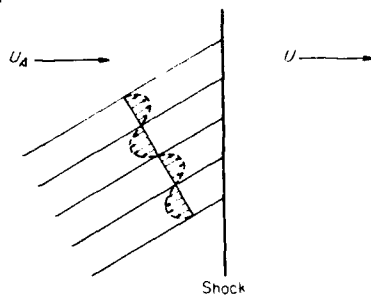
<sup>1</sup> Supersedes NACA TN 3255, "Shock-Turbulence Interaction and the Generation of Noise," by H. S. Ribner, 1954.

ing motion (e. g., ref. 9); a portion of such a wave is shown in perspective in sketch (a):



(a) Wave of shearing motion.

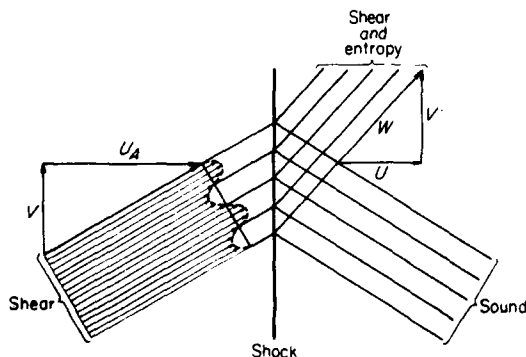
A similar wave encountering a shock is shown schematically in sketch (b),



(b) Convection of shear wave through shock: original unsteady-flow problem.

the wave and the shock being viewed "edge-on." The wave-shock interaction is analyzed in reference 2, and what follows first is a brief physical account of the main results. The wave is supposed to be convected downstream by the mainstream with velocity  $U_A$  so that it passes through the shock. The passage is evidently an unsteady process, since the intercepts of the inclined lines—the planes of constant phase or wave fronts—move downward along the shock; it can be shown that a sinusoidal disturbance ripple will move along the shock with the same speed  $V$ .

The unsteady-flow problem may be treated directly (ref. 4), or it may be converted to an equivalent steady-flow problem by superposing an upward velocity  $V$  (ref. 2). The conversion is illustrated in sketch (c):



(c) Transformation to steady-flow problem by superposition of velocity  $V$ .

The cross velocity  $V$  therein has been chosen so that the resultant stream velocity is parallel to the wave fronts in the shear wave; the observer then sees what appears to be a steady sinusoidal shear flow passing through an oblique shock. This may be called the equivalent oblique shock. (Addition of the upward velocity  $V$  is, of course, equivalent to transforming to a moving frame of reference.)

Downstream of the shock, the resultant stream flow is deflected according to the laws for oblique shocks; the streamlines are the upper lines in the sketch. The vorticity of the initial shear wave is convected along these streamlines together with the additional vorticity generated by the shock. The net result is a refracted, amplified shear wave aligned with these streamlines. The angle of refraction is just the angle of flow deflection of the oblique shock.

Superposed on the refracted shear wave is an entropy wave of the same inclination and wave length. This wave arises from the convection of entropy perturbations generated at the shock, precisely as the shear wave results from the convection of vorticity. The entropy wave is manifested physically as a spatial variation of temperature and density at constant pressure, by virtue of the equation of state.

The nonuniform velocity in the shear flow results in a nonuniform pressure jump across the shock. The ultimate effect is that the shock front develops ripples, modifying the pressure variations, and the resultant pressure variations propagate downstream as a plane sinusoidal wave (lower lines in sketch (c)).

The character of this wave depends on whether the resultant velocity  $W$  behind the equivalent oblique shock is subsonic or supersonic; this in turn depends on the initial wave inclination through  $V$ . When  $W$  is supersonic, the pressure wave is a plane sinusoidal sound wave; it appears as a stationary Mach wave pattern in the steady-flow reference frame. When  $W$  is subsonic, it may be shown that the pressure wave, while still plane, is not a simple sound wave, but rather attenuates exponentially with distance downstream of the shock; the resultant disturbance velocity is not normal to the wave front, and the wave propagates relative to the surrounding fluid at less than sonic speed.

#### QUANTITATIVE DISCUSSION

**Elementary wave.** Thus far the waves have been discussed only qualitatively. Elementary spectrum waves of this sort may be expressed quantitatively in the form

$$d\alpha = dZ_0 e^{i(kx - \omega t)} \quad (1)$$

(All symbols are defined in appendix A.) The wave-number vector  $\underline{k}$  is directed normal to the wave fronts and its magnitude equals  $2\pi$ /wave length. The wave amplitude is given by the complex quantity  $dZ_0$ . When  $\alpha$  stands for temperature, pressure, density, or entropy, these are simple scalar waves. When  $\alpha$  stands for the components  $u, v, w$  of the velocity, these are vector waves; two cases may then be distinguished: the waves are either irrotational and compressible (sound waves) or rotational and incompressible (vorticity waves). (See, e. g., ref. 10.) In the first case the irrotationality condition  $\text{curl } \underline{g} = 0$  requires that the velocity  $\underline{g}$  and wave vector  $\underline{k}$  be parallel ( $u, v, w$  proportional to  $k_1, k_2, k_3$ , respectively); the sound waves are thus longi-

tudinal. In the second case the incompressibility condition  $\text{div } \underline{u} = 0$  requires that the velocity  $\underline{u}$  and the wave vector  $\underline{k}$  be perpendicular; that is,

$$k_1 u + k_2 v + k_3 w = 0 \quad (2)$$

Thus, the vorticity waves are transverse and have the character of a shearing motion (see sketch (a)); in the discussion they have been referred to as "shear waves."

**Geometric reexamination of prior results.**—The shock-interaction process for a single shear wave is given quantitatively in reference 2, but the results are formulated in two dimensions. It will be necessary to reexamine the problem geometrically in order that the results may be reexpressed in three dimensions.

A perspective view of the initial shear wave in the new  $x_1, x_2, x_3$ -coordinate system is shown in figure 1. The portion of the shear wave shown is on the downstream side of the shock front, which is identified with the  $x_2, x_3$ -plane. A plane passed through the  $x_1$ -axis perpendicular to the wave fronts cuts the shock in the line  $Or$ . At a given instant of time this  $x_1, r$ -plane corresponds precisely to what is called the  $x, y$ -plane in reference 2. The angle  $\varphi$  of the  $x_1, r$ -plane with the horizontal is then the third coordinate in a system of cylindrical coordinates.

In reference 2 the time was eliminated from the equations by employing a frame of reference moving with a velocity  $V$  downward along the shock front, the so-called steady-flow frame of reference. In the present paper all results refer to a definite instant of time,  $t=0$ . Thus, motion of the reference frame plays no part, and the results of the earlier paper carry over to the present coordinate system on simply

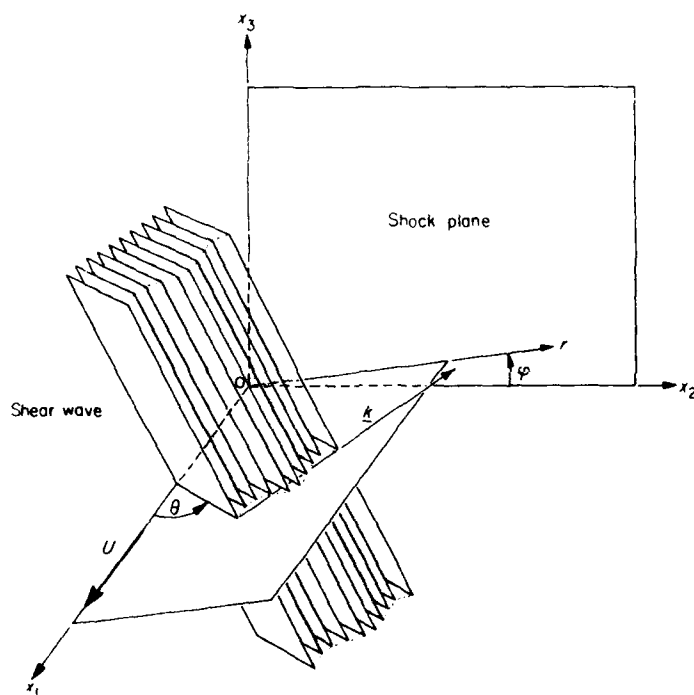


FIGURE 1. Perspective view of shear wave in relation to reference frame.

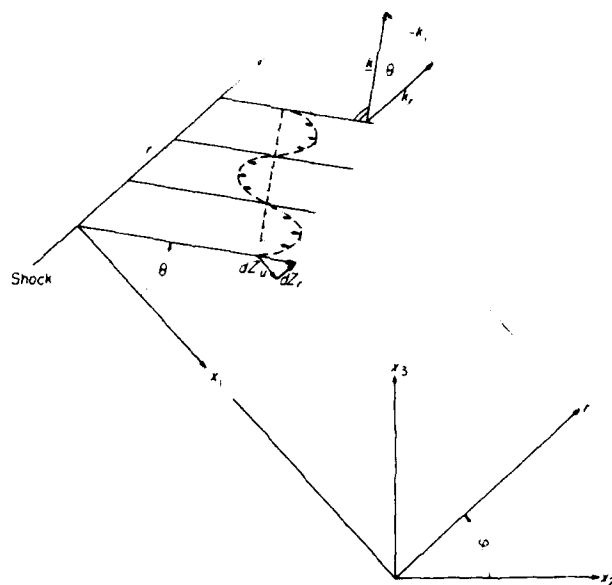


FIGURE 2. Projective view of shear wave in relation to reference frame

replacing  $x, y$  by  $x_1, r$ , respectively. The results of the transformation are given in the following sections with the disturbances reexpressed in nondimensional form according to the scheme

$u, v, w$  = components of velocity perturbation critical speed of sound  $a^*$

$p$  = pressure perturbation mean static pressure

$\rho$  = density perturbation mean density

$\tau$  = temperature perturbation mean temperature

In addition, there are other minor respects in which the notation has been modified from that of reference 2; for example, the waves are expressed in complex form.

**Initial shear wave (~ initial turbulence).**—At time  $t=0$ , the velocity field of the initial shear wave is, in cylindrical coordinates,

$$\left. \begin{aligned} du &= dZ_u e^{ik \cdot x} \\ dr_r &= dZ_r e^{ik \cdot x} \\ dr_\phi &= dZ_\phi e^{ik \cdot x} \end{aligned} \right\} \quad (3)$$

where  $du$  is parallel to  $x_1$  (longitudinal direction),  $dr_r$  is parallel to  $r$ , and  $dr_\phi$  is perpendicular to  $r$  and  $x_1$ , in the direction of increasing  $\varphi$  (see figs. 1 and 2). The wave-number vector  $\underline{k}$  lies in the  $x_1, r$ -plane, making an angle  $\theta$  with the  $r$ -axis.

**Refracted shear-entropy wave (~ final turbulence and entropy spottiness).**—The velocity field of the refracted shear wave (fig. 3) is

$$\left. \begin{aligned} du' &= dZ'_u e^{ik' \cdot x} & dZ'_u &= X dZ_u \\ dr'_r &= dZ'_r e^{ik' \cdot x} & dZ'_r &= Y dZ_r \\ dr'_\phi &= dZ'_\phi e^{ik' \cdot x} & dZ'_\phi &= dZ_\phi \end{aligned} \right\} \quad (4)$$

at time  $t=0$ , where  $\underline{k}'$  is the new wave-number vector, making an angle  $\theta'$  with the  $r$ -axis. The radial components of  $\underline{k}'$

and  $\underline{k}$  are equal ( $k'_r = k_r$ ), and the further dependence of  $\underline{k}'$  on  $\underline{k}$  is expressed through the dependence of  $\theta'$  on  $\theta$ . Similarly, the complex amplification factors  $X$  and  $Y$  depend on  $\underline{k}$  in terms of  $\theta$ . Expressions for  $X$ ,  $Y$ , and  $\theta'$  are given in appendix A.

The perturbation pressure  $dp'$  will be zero because this is again a shear wave, free of accelerations. The temperature perturbation associated with the companion entropy wave (fig. 3) will be

$$d\tau' = dZ'_e e^{ik'_r x} \quad dZ'_e = T dZ_u \quad (5)$$

With  $p' = 0$  (to the first order), the dimensionless density perturbation  $\rho'$  will be just the negative of the dimensionless temperature perturbation  $\tau'$ , according to the linearized equation of state. The form of the function  $T$  is given in appendix A.

Aside from the change in wave inclination, the description of the refracted shear-entropy wave in terms of the initial shear wave depends entirely on the amplification factors  $X$  and  $Y$  and the function  $T$ . Such functions play a role similar to the "transfer functions" of the theory of servomechanisms (ref. 11), and it appears appropriate to carry the name over to the present field.

**Generated sound wave** ( $\sim$  noise field).—The shear-entropy wave downstream of the shock is accompanied by a plane irrotational pressure wave (sound wave) of different inclination (see fig. 3). For small inclinations  $\theta$  of the initial shear wave, this pressure wave attenuates exponentially with distance from the shock; for inclinations greater than a certain critical value  $\theta_{cr}$  (see appendix A), the pressure wave is unattenuated. The critical wave inclination  $\theta_{cr}$  corresponds to the attainment of sonic speed in the mean flow behind the "equivalent oblique shock" referred to in the qualitative discussion.

The velocity field can be represented in the form

$$\left. \begin{aligned} du'' &= dZ''_u e^{ik''_r x} & dZ''_u &= \chi dZ_u \\ dv''_r &= dZ''_r e^{ik''_r x} & dZ''_r &= T dZ_u \\ dv''_\phi &= dZ''_\phi e^{ik''_r x} & dZ''_\phi &= 0 \end{aligned} \right\} \quad (6)$$

where  $\underline{k}''$  is the wave-number vector, making an angle  $\theta''$  with the  $x$ -axis; again the radial component matches that of  $\underline{k}$ ; namely,  $k''_r = k_r$ . The sound-wave angle  $\theta''$  and the transfer functions  $\chi$  and  $T$  are specified functions of the shear-wave angle  $\theta$ ; moreover, for  $0 \leq \theta < \theta_{cr}$ ,  $\chi$  and  $T$  are functions of  $x_1$ , showing an exponential decay to zero as  $x_1 \rightarrow \infty$ .

The pressure perturbation may be written

$$dp'' = dZ''_p e^{ik''_r x} \quad dZ''_p = P dZ_u \quad (7)$$

where  $P = P(x_1)$  is a transfer function defined in appendix A; like  $\chi$  and  $T$ ,  $P$  decays exponentially with  $x$  for  $0 \leq \theta < \theta_{cr}$ . The corresponding density and temperature perturbations are proportional to  $p''$ ; they may be obtained from the isentropic property of the sound wave as  $\rho'' = p''/\gamma$  and  $\tau'' = p''(\gamma - 1)/\gamma$ .

**Transformation to Cartesian coordinates.**—Expressions for the velocity field in Cartesian coordinates will be needed. The transformation from cylindrical coordinates is effected by means of the relations

$$\left. \begin{aligned} dZ_r &= dZ_r \cos \varphi - dZ_\phi \sin \varphi \\ dZ_\phi &= dZ_r \sin \varphi + dZ_\phi \cos \varphi \end{aligned} \right\} \quad (8)$$

where primes ( $\sim$  refracted shear wave) or double primes ( $\sim$  sound wave) may be inserted throughout as needed.

The transformation results in

$$\text{Initial shear} \left\{ d\alpha = dZ_\alpha e^{ik''_r x}, \text{ where } \alpha = u, r, \phi \right\} \quad (9)$$

$$\text{Final Shear} \left\{ \begin{aligned} d\alpha' &= dZ'_\alpha e^{ik''_r x}, \text{ where the values of } dZ'_\alpha \\ &\text{for } \alpha = u, r, \phi \text{ are, respectively,} \\ dZ'_u &= X dZ_u \\ dZ'_r &= Y dZ_r \cos \varphi - dZ_\phi \sin \varphi \\ dZ'_\phi &= Y dZ_r \sin \varphi + dZ_\phi \cos \varphi \end{aligned} \right\} \quad (10)$$

$$\text{Sound} \left\{ \begin{aligned} d\alpha'' &= dZ''_\alpha e^{ik''_r x}, \text{ where the values of } dZ''_\alpha \\ &\text{for } \alpha = u, r, \phi \text{ are, respectively,} \\ dZ''_u &= \chi dZ_u \\ dZ''_r &= T dZ_r \cos \varphi \\ dZ''_\phi &= T dZ_r \sin \varphi \end{aligned} \right\} \quad (11)$$

#### SPECTRAL ANALYSIS OF RANDOM FIELDS

The foregoing relations will be fitted later into a spectral analysis of the fields of turbulence and noise. Appropriate analytical techniques can be found in the spectral theory of random functions; suitable developments of this sort are given by, for example, Moyal (ref. 10) and Batchelor (ref. 12) for spatially homogeneous fields. The first part of the present section will be devoted to an interpretation (with some liberties) of relevant parts of the two papers; the latter part will be devoted to developments for inhomogeneous fields and for correlations of a two-dimensional field with a three-dimensional field.

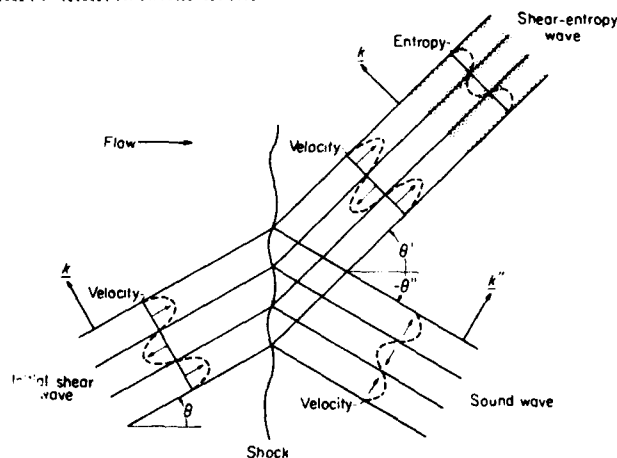


FIGURE 3. Interaction of shear wave with shock: view in  $x_1, r$ -plane.

## HOMOGENEOUS FIELDS

**Amplitude spectra.** Consider a three-dimensional field of small disturbance (e. g., turbulence or noise) of unlimited extent. Let this field be homogeneous in the sense that the statistical properties do not vary from point to point. The instantaneous spatial distribution of any physical quantity  $\alpha$  can then be represented mathematically by a Fourier integral in the Stieltjes form (refs. 10 and 12)

$$\alpha(\underline{x}) = \int e^{i\underline{k} \cdot \underline{x}} dZ_\alpha(\underline{k}) \quad (12)$$

where the triple integral goes from  $-\infty$  to  $\infty$  in each component of  $\underline{k} = (k_1, k_2, k_3)$ .

If equation (12) is written in the form

$$\alpha = \int d\alpha(\underline{k})$$

then, by comparison with equation (1),  $d\alpha$  can be identified with what has been called an elementary spectrum wave. The Fourier integral is thus to be interpreted as a superposition of infinitely many of such plane waves. In the integral the components of  $\underline{k}$  take on all values; it follows from the significance of  $\underline{k}$  as a wave-number vector that all wave inclinations and wave lengths appear. An aggregate of vorticity waves with a suitable distribution of amplitudes among the various wave lengths and inclinations can represent a turbulent field (ref. 13). Similarly, an aggregate of sound waves suitably distributed can represent a random noise field (ref. 10). Finally, an aggregate of the scalar entropy waves can represent a random field of entropy spottiness. A combination of these three basic types of disturbance—entropy spottiness, turbulence, and noise—constitutes the most general random small-disturbance field that may exist in a gas (refs. 4 and 5).

**Correlations.**—Let  $\alpha$  be measured at some point  $P$  and  $\beta$  at some point  $\hat{P}$  a vector distance  $\underline{\xi}$  from  $P$ ; then the space average of the product  $\alpha\beta$  as  $\hat{P}$  and  $P$  vary but their vector separation  $\underline{\xi}$  is held fixed may be defined as the space-average correlation  $\overline{\alpha\beta}(\underline{\xi})$ . Alternatively, the disturbance field may be considered to be just one of a large number, or ensemble, of statistically similar fields (e. g., the flow fields of a great many "identical" wind tunnels operated simultaneously); the average of  $\alpha\beta$ , with  $P$  and  $\hat{P}$  fixed, over all members of the group, is the ensemble-average correlation. The equations that follow, from the theory of random functions, refer solely to ensemble averages, but space averages are desired in practical applications. The ergodic hypothesis of probability theory equates the space average to the ensemble average provided that, at any instant, the disturbance fields  $\alpha$  and  $\beta$  are stationary random functions of position; that is, the disturbance fields are spatially homogeneous.

In what follows, the term "cross-correlation" will be applied for  $\alpha \neq \beta$ , the term "self-correlation," or simply "correlation," for  $\alpha = \beta$ .

**Correlation and power spectra.**—The cross-correlation  $\overline{\alpha\beta}(\underline{\xi})$  (like  $\alpha$  or  $\beta$ , individually: see eq. (12)) may be ex-

pressed by means of the Fourier integral as a spectrum of plane sine waves:

$$\overline{\alpha\beta}(\underline{\xi}) = \int e^{i\underline{k} \cdot \underline{\xi}} |\alpha\beta| d\underline{k} \quad (13)$$

where  $|\alpha\beta|$  is a function of  $\underline{k}$ , and  $d\underline{k}$  is an abbreviation for  $dk_1 dk_2 dk_3$ . The differential  $e^{i\underline{k} \cdot \underline{\xi}} |\alpha\beta| d\underline{k}$  may be regarded as the contribution to the correlation made by spectrum components with wave number between  $\underline{k}$  and  $\underline{k} + d\underline{k}$ . The function  $|\alpha\beta|$  is called the "spectral density" when  $\alpha = \beta$ , the "cross-spectral density" when  $\alpha \neq \beta$  (ref. 11). The array of nine spectral densities signified by  $|\alpha\beta|$  when  $\alpha$  and  $\beta$  are limited to mean  $u$ ,  $v$ , or  $w$  is the "spectral tensor" of the velocity field and is commonly written as  $\Gamma_{ij}$  or  $\Phi_{ij}$ . (The corresponding array of the nine velocity correlations  $\overline{\alpha\beta}(\underline{\xi})$  is the "correlation tensor," commonly written as  $R_{ij}(\underline{\xi})$ .)

Equation (13) includes as a special case the self-correlation or mean-square relation

$$\overline{\alpha^2} = \int |\alpha\alpha| d\underline{k}, \quad \text{where } \underline{\xi} = 0 \quad (14)$$

If  $\alpha$  were a velocity component (say  $u$ ), then  $\overline{\alpha^2}$  would be twice the space-average kinetic energy per unit mass associated with  $u$ . The spectral density  $|\alpha\alpha|$  is in this case an energy density (per unit mass, per unit wave number). For similar reasons, where spectra of the kind defined by equation (14) have occurred in physics (e. g., in the harmonic analysis of radio noise), they have generally been called energy, intensity, or power spectra.

**Correlation spectrum in terms of amplitude spectra.**

The rather analogous forms of equations (12) and (13) are of interest. Equation (12) expresses the spectrum of the amplitude of the fluctuating quantity  $\alpha$ ; this may be termed an amplitude spectrum. Equation (13) expresses the spectrum of the correlation of  $\alpha$  with  $\beta$ ; this has been termed a correlation spectrum. The complex magnitude  $dZ_\alpha(\underline{k})$  of the amplitude spectrum fluctuates in an apparently random manner as  $\underline{k}$  is varied (refs. 10 and 12). The magnitude  $|\alpha\beta| d\underline{k}$  of the correlation spectrum, on the other hand, varies smoothly with  $\underline{k}$ , since the correlation is a smoothed or averaged quantity (ref. 12). The amplitude spectrum gives no direct information concerning averaged (i. e., statistical) properties of the disturbance field, whereas the correlation spectrum leads directly to expressions for correlations and mean-square values (see eqs. (3) and (4)). One-dimensional spectra and scales of turbulence can also be determined (e. g., ref. 14).

It would be desirable to formulate the shock-turbulence interaction problem directly in terms of correlation spectra, but formidable difficulties stand in the way. It has been simpler to start with the shock interaction of a single shear wave, which deals with amplitude spectra, and to infer from this the changes in the correlation spectra. The whole procedure depends on the following relation (refs. 10 and 12) which connects the two kinds of spectra, namely,

$$|\alpha\beta| d\underline{k} = dZ_\alpha^*(\underline{k}) dZ_\beta(\underline{k}) \quad (15)$$



where  $dZ(\underline{k})$  is associated with the wave-number range between  $\underline{k}$  and  $\underline{k} + d\underline{k}$ , and the bar represents the ensemble average. This relation is fundamental to the spectrum analysis of the present paper. Its significance is this: the single-wave analysis (summarized in an earlier section) provided the change in amplitude of an individual spectrum wave in the form  $dZ_a \rightarrow dZ'_a$ , say, and similarly,  $dZ_b \rightarrow dZ'_b$ ; equation (15) provides the means for determining therefrom the corresponding change in the spectral density:  $[\alpha\beta] \rightarrow [\alpha'\beta']$ .

#### INHOMOGENEOUS FIELDS

The spectral representation of a spatially homogeneous random field is given by equation (12):

$$\alpha(\underline{x}) = \int e^{i\underline{k} \cdot \underline{x}} dZ_a(\underline{k})$$

A corresponding possible representation of an inhomogeneous field is

$$\alpha(\underline{x}) = \int e^{i\underline{k} \cdot \underline{x}} dZ_a(\underline{k}, \underline{x}) \quad (16)$$

where  $dZ_a$  now depends on position; the sound field behind the shock is of this character. The following spectral analysis of such inhomogeneous fields is a development of Moyal's treatment of homogeneous fields (ref. 10).

Let  $\alpha(\underline{x})$  and  $\beta(\underline{x}')$  be inhomogeneous fields

$$\alpha(\underline{x}) = \int e^{i\underline{k} \cdot \underline{x}} dZ_a^*(\underline{k}, \underline{x}) \quad (17)$$

$$\beta(\underline{x}') = \int e^{i\underline{k}' \cdot \underline{x}'} dZ_b(\underline{k}', \underline{x}') \quad (18)$$

where equation (17) is an alternate form of equation (16). The correlation of  $\alpha$  and  $\beta$  for fixed positions  $\underline{\hat{x}}$  and  $\underline{\hat{x}}'$ , respectively, can be formed by taking the ensemble average of their product:

$$\overline{\alpha(\underline{\hat{x}})\beta(\underline{\hat{x}}')} = \iint e^{i\underline{k} \cdot \underline{\hat{x}} + i\underline{k}' \cdot \underline{\hat{x}}'} dZ_a^*(\underline{k}, \underline{\hat{x}}) dZ_b(\underline{k}', \underline{\hat{x}}') \quad (19)$$

The operations of integration and averaging commute, so the averaging bar may be regarded as placed over the  $dZ$ 's alone on the right side.

Equation (19) could immediately be simplified if the fields  $\alpha(\underline{x})$  and  $\beta(\underline{x}')$  were homogeneous; in that case the important relation

$$\overline{dZ_a^*(\underline{k})dZ_b(\underline{k}')} = [\alpha\beta] d\underline{k} d\underline{k}' \delta(\underline{k}' - \underline{k}) \quad (20)$$

where

$$\delta(\underline{k}' - \underline{k}) = 0 \text{ for } \underline{k}' \neq \underline{k}$$

$$= \infty \text{ for } \underline{k}' = \underline{k}$$

and

$$\int_{-\infty}^{\infty} \delta(\underline{k}' - \underline{k}) d\underline{k}' = 1$$

would hold (ref. 10), according to the spectral theory of

random functions. The simplification can still be achieved by replacing the inhomogeneous fields by "equivalent" homogeneous fields that match, respectively, at the points  $\underline{\hat{x}}$  and  $\underline{\hat{x}}'$ . This is accomplished by freezing  $dZ_a^*(\underline{k}, \underline{x})$  in equation (17) at the value  $dZ_a^*(\underline{k}, \underline{\hat{x}})$  while allowing  $\underline{x}$  to vary in the exponential, and correspondingly freezing  $dZ_b$  in equation (18).

When applied to the so-defined equivalent homogeneous fields, equation (20) reads

$$\overline{dZ_a^*(\underline{k}, \underline{\hat{x}})dZ_b(\underline{k}', \underline{\hat{x}}')} = [\alpha\beta] d\underline{k} d\underline{k}' \delta(\underline{k}' - \underline{k}) \quad (21)$$

where the  $\sim$  over  $[\alpha\beta]$  signifies the functional dependence on  $\underline{\hat{x}}$  and  $\underline{\hat{x}}'$ . Upon substitution into equation (19) and integration over  $\underline{k}'$  there results, with  $\underline{\hat{x}} = \underline{\hat{x}}' = \underline{\hat{x}}$ ,

$$\overline{\alpha(\underline{\hat{x}})\beta(\underline{\hat{x}}')} = \int e^{i\underline{k} \cdot \underline{\hat{x}}} [\alpha\beta] d\underline{k} \quad (22)$$

The spectral density  $[\alpha\beta]$  can be evaluated by integrating equation (21) over  $\underline{k}'$ :

$$[\alpha\beta] d\underline{k} = \overline{dZ_a^*(\underline{k}, \underline{\hat{x}})dZ_b(\underline{k}, \underline{\hat{x}}')} \quad (23)$$

where the integral property of the  $\delta$ -function,

$$\int_{-\infty}^{\infty} f(\underline{k}') \delta(\underline{k}' - \underline{k}) d\underline{k}' = f(\underline{k})$$

has been used, with  $f(\underline{k}')$  an arbitrary function.

Equations (22) and (23) for inhomogeneous fields are of the same form as their counterparts, equations (13) and (15), respectively, for homogeneous fields. In the homogeneous case the  $dZ$ 's are functions of position, and equation (23) implies a corresponding dependence of  $[\alpha\beta]$  on position. Moreover, the correlation  $\overline{\alpha(\underline{\hat{x}})\beta(\underline{\hat{x}}')}$  depends on  $\underline{\hat{x}}$  and  $\underline{\hat{x}}'$  separately as well as on their separation  $\underline{\hat{x}}$ .

#### CORRELATION OF TWO-DIMENSIONAL FIELD WITH THREE-DIMENSIONAL FIELD

The local perturbations of the shock face from the mean  $(x'_2, x'_3)$  plane constitute a homogeneous two-dimensional field of the general form

$$\beta(\hat{x}'_1, x'_2, x'_3) = \int e^{i\underline{k}(\hat{x}'_1 - x'_2)\underline{\hat{x}}_1} dW_b(k'_2, k'_3) \quad (24)$$

where  $x'_1$  has been fixed at the value  $\hat{x}'_1$ . It may be desired to correlate such a field locally with a three-dimensional field (e. g., the turbulent velocity field). To this end, equation (24) is rewritten in the form

$$\beta(\underline{x}') = \int e^{i\underline{k}' \cdot \underline{x}'} \left[ e^{-i\underline{k}'_1 \hat{x}'_1} dW_b(k'_2, k'_3) \right]$$

Now, if  $x'_1$  in  $e^{-i\underline{k}'_1 \hat{x}'_1}$  is fixed at the value  $\hat{x}'_1$ ,  $\beta$  will be generalized to a three-dimensional field (elementary wave number  $\underline{k}'$ ) that matches the original two-dimensional field in its

plane of definition  $x_1 = \hat{x}_1$ . This "equivalent" field may be written

$$\left. \begin{aligned} \beta(\underline{x}') &= \int e^{i\mathbf{k}' \cdot \underline{x}'} dZ_3(\underline{k}') \\ \text{where} \quad dZ_3(\underline{k}') &= e^{-i\mathbf{k}' \cdot \underline{x}'} dW_3(k'_1, k'_2, k'_3) \end{aligned} \right\} \quad (25)$$

Equation (25) is of the form of a three-dimensional homogeneous field and may be used in place of (24) in equations (13) and (15) to provide the correlation of  $\beta$  with any three-dimensional homogeneous field in the common plane  $x_1 = \hat{x}_1$ .

### SHOCK INTERACTION OF SPECTRUM OF SHEAR WAVES TURBULENCE

The interaction of a single shear wave with a shock has been discussed in detail. With this as the basis, the statistical behavior of a spectrum of shear waves representing turbulence will now be derived; the procedure will make use of the spectral-analysis relations of the last section. The problem is formulated as follows: given the spectra (and hence correlations and mean-square values) associated with the turbulence convected into the shock, to calculate therefrom the spectra, correlations, and mean-square values associated with the turbulence, entropy spottiness, and noise in the flow downstream of the shock.

#### DIAGONAL TERMS OF VELOCITY SPECTRUM TENSOR

The respective spectrum tensors for the turbulence and noise downstream of the shock each consist of nine elements; of these the three diagonal terms are most important since they lead to the mean squares of the velocity components. The relatively simple derivation of the first diagonal term and the sum of the second and third will be carried out in the present section. The derivation of the complete tensor is carried out in appendix B by a more formal procedure.

**Turbulence field.** The shock interaction effects have been expressed in terms of relations between wave amplitudes on opposite sides of the shock (eqs. (9) and (10)). Corresponding relations between spectral densities (elements) on the two sides can be obtained by use of equation (17). Some preliminary manipulation is required; thus multiply both sides of equations (10) by their complex conjugates, and add the last two; there results

$$dZ_u'^* dZ_u' = X^2 dZ_u^* dZ_u \quad (26)$$

$$dZ_v'^* dZ_v' + dZ_w'^* dZ_w' = Y^2 dZ_v^* dZ_v + dZ_w^* dZ_w \quad (27)$$

But by geometry (fig. 2),

$$dZ_v = dZ_u \tan \theta$$

$$dZ_v^* = dZ_u^* \tan \theta$$

and also, by the coordinate transformation (8),

$$dZ_v^* dZ_v + dZ_w^* dZ_w = dZ_v^* dZ_v + dZ_w^* dZ_w$$

Thus, equation (27) becomes

$$dZ_v'^* dZ_v' + dZ_w'^* dZ_w' = (Y^2 - 1) \tan^2 \theta dZ_v^* dZ_v + dZ_v^* dZ_v + dZ_w^* dZ_w \quad (28)$$

Application of equation (15) yields

$$\left. \begin{aligned} |u'u'| d\underline{k}' &= X^2 |uu| d\underline{k} \\ |v'v'| + |w'w'| d\underline{k}' &= (Y^2 - 1) \tan^2 \theta |uu| d\underline{k} + |uu| d\underline{k} \end{aligned} \right\} \quad (29)$$

These are the desired expressions relating diagonal elements of the spectrum tensors of the turbulence on opposite sides of the shock.

**Noise field.** If operations similar to those of the last section are applied to equations (11), there results

$$\left. \begin{aligned} |u''u''| d\underline{k}'' &= X^2 |uu| d\underline{k} \\ |v''v''| + |w''w''| d\underline{k}'' &= Y^2 \tan^2 \theta |uu| d\underline{k} \end{aligned} \right\} \quad (30)$$

These equations relate the diagonal elements of the spectrum tensor of the noise generated behind the shock to the longitudinal spectral density of the initial turbulence ahead of the shock.<sup>2</sup>

#### MEAN-SQUARE VELOCITY COMPONENTS

**Turbulence field.** The mean-square velocity components follow directly from integration of the spectral density (see eq. (14)). Integration of both sides of equations (29) yields

$$\left. \begin{aligned} \overline{u'^2} &= \int X^2 |uu| d\underline{k} \\ \overline{v'^2} + \overline{w'^2} &= \overline{v^2} + \overline{w^2} + \int (Y^2 - 1) \tan^2 \theta |uu| d\underline{k} \end{aligned} \right\} \quad (31)$$

Thus, the mean-square velocity components behind the shock (primed values) are given in terms of those ahead of the shock, the single-wave transfer functions  $X$  and  $Y$ , and the longitudinal spectral density  $|uu|$  of the initial turbulence. Note that  $X$  and  $Y$  are functions of  $k$  in terms of  $\theta$  (see appendix A).

**Noise field.** Similarly, integration of equations (30) yields the mean-square velocity components in the noise field:

$$\left. \begin{aligned} \overline{u''^2} &= \int X^2 |uu| d\underline{k} \\ \overline{v''^2} + \overline{w''^2} &= \int Y^2 \tan^2 \theta |uu| d\underline{k} \end{aligned} \right\} \quad (32)$$

Here again,  $X$  and  $Y$  are functions of  $k$  in terms of  $\theta$ .

<sup>2</sup> Direct expressions for the spectra downstream of the shock may be desired, free of the unequal volume elements  $d\underline{k}$ ,  $d\underline{k}'$ , or  $d\underline{k}''$ . This may be effected in eq. (29) by dividing both sides by  $d\underline{k}'$ , then (since  $d\underline{k}$  is shorthand for  $dk_1 dk_2 dk_3$ , and similarly for  $d\underline{k}'$ ) the ratio  $d\underline{k} d\underline{k}'$  may be interpreted as the Jacobian (say  $J'$ ) for the transformation from  $k$  to  $k'$ . Upon evaluation

$$J' = \frac{1}{m}$$

Similarly, in eq. (30) divide by  $d\underline{k}''$  and interpret  $d\underline{k} d\underline{k}''$  as the Jacobian (say  $J''$ ) for the transformation from  $k$  to  $k''$ . Upon evaluation

$$J'' = \frac{\cos^2 \theta''}{m \cos^2 \theta'} \frac{\partial \theta'}{\partial \theta''}$$

## MEAN-SQUARE PRESSURE

The first-order pressure field is associated solely with the noise field; the pressure field associated with the turbulence is of the second order in velocity and may be neglected in comparison. The spectral density of the noise pressure can be related to the spectral density of the longitudinal velocity in the initial turbulence; the relation is obtained by multiplying both sides of the second of equations (7) by their complex conjugates, averaging, and applying equation (15) to each side:

$$\overline{p''p''} dk_{\xi}'' = P^{-1} \overline{u u} dk_{\xi} \quad (63)$$

The integration of both sides of equation (63) yields the mean-square pressure in the noise field as

$$\overline{p''^2} = \int P^{-1} \overline{u u} dk_{\xi} \quad (64)$$

## MEAN-SQUARE TEMPERATURE

The temperature perturbations in the noise field, because of the isentropic relation, are equal to  $(\gamma - 1)/\gamma$  times the pressure perturbations; thus, the relations corresponding to equations (63) and (64) may be written down at once:

The temperature perturbations associated with the entropy-spottiness behind the shock require a separate analysis. The spectral density of the temperature perturbations can be evaluated by operating on equation (5) in the now-familiar manner (see remarks preceding eq. (63)); the result is

$$\overline{\tau''\tau''} dk_{\xi}'' = T^{-1} \overline{u u} dk_{\xi} \quad (65)$$

The integral relation obtained from equation (65) is

$$\overline{\tau''^2} = \int T^{-1} \overline{u u} dk_{\xi} \quad (66)$$

This equation evaluates, for the region behind the shock, that part of the mean-square temperature spottiness associated with the entropy spottiness.

## MEAN-SQUARE DENSITY

It is unnecessary to write down special expressions for the density field; the respective contributions of entropy spottiness and noise to the density perturbations are related to the corresponding temperature and pressure perturbations by  $\rho'' = \tau''$  and  $\rho''/\gamma$ , according to the small-perturbation form of the equation of state.

## CORRELATIONS NOT JOINTLY INVOLVING TURBULENCE AND NOISE

**Attempts at simplification.** If the spectral density  $\overline{u u}(k)$  is known, the corresponding two-point correlation  $\overline{u u}(\xi)$  can, in principle, be obtained by means of equation

(14). In this fashion, for example, the long correlation in the turbulence behind the shock may be expressed, with use of equation (20), as

$$\overline{u' u'}(\xi') = \int N^{-1} \overline{u u} e^{i k' \xi'} dk_{\xi} \quad (67)$$

or

$$\int N^{-1} \overline{u u} e^{i k' \xi'} dk_{\xi} = J' dk_{\xi} \quad (68)$$

(See footnote 2, p. 7, for significance of  $J'$ .)

Either of the forms (67) or (68) may be used because of the admixture of  $k$  and  $k'$  in the  $\overline{u u}$  is ordinarily most simply expressed as  $\overline{u u}(k)$ . However, it is possible to find a fixed vector  $k'$  that satisfies the relation  $k' \cdot \xi' = k \cdot \xi$ ; this gives the relation

$$\overline{u' u'}(\xi') = \int N^{-1} \overline{u u} e^{i k' \xi'} dk_{\xi} \quad (69)$$

where  $k' = u \xi'$ ,  $k = \xi'$ ,  $k' \cdot \xi' = k \cdot \xi$ . In all the correlations involving properties of the entropy-spottiness behind the shock, where the velocity components, temperature, density, transformation  $k' \cdot \xi' = k \cdot \xi$  can be made to be exponential.

The physical interpretation of the relation  $\xi'$  is this: if two fluid particles upstream of the shock are a vector distance  $\xi$  apart, after convection to the shock they will be a vector distance  $\xi'$  apart. The "box" of turbulent fluid of edges  $\xi_1, \xi_2, \xi_3$  will on passing through the shock and will emerge as a shorter box of edges  $\xi'_1, \xi'_2, \xi'_3$ . Therefore, equation (69) in effect expresses correlations in the space downstream of the shock in terms of equivalent correlations in the space upstream of the shock.

The analog of equation (67) for the correlations of the noise field involves  $k'' \cdot \xi''$  in it rather than  $k' \cdot \xi'$ . Here no great simplification is possible in general; there exists no fixed vector  $k''$  that satisfies the relation  $k'' \cdot \xi'' = k \cdot \xi$ . This is because of the nature of the transformation from  $k$  to  $k''$ ; the components of the two vectors are not in fixed proportion but instead vary with the inclination of  $k$ . A coordinate compression  $\xi \rightarrow \xi'$  that works for the coordinate compression  $k \rightarrow k'$  that works for the field (it expresses the change in dimensions of the convected through the shock) will not work for the noise field. An exception occurs when  $\xi''$  is chosen parallel to the shock plane (radial direction,  $x_1 = 0$ ). Then  $k'' = k$ , and since  $k'' = k$ , it follows that for this case  $k'' \cdot \xi'' = k \cdot \xi$ .

The integral for a particular correlation simplifies considerably when  $\xi$  (or  $\xi'$ , or  $\xi''$ ) is taken in the

direction of the velocity  $u$  may be

backward and the direction of  $k$  is at an angle to the direction of  $u$  that satisfies the condition

on cross-correlation and they be entropy-spottiness; the multiply the

between  $\xi$  and the shock are a vector distance  $\xi'$  apart. The other way, a compressed turbulent fluid "box" upstream as a function of the distance in the space

of properties of the noise field involves  $k'' \cdot \xi''$  in it rather than  $k' \cdot \xi'$ . Here no great simplification is possible in general; there exists no fixed vector  $k''$  that satisfies the relation  $k'' \cdot \xi'' = k \cdot \xi$ . This is because of the nature of the transformation from  $k$  to  $k''$ ; the components of the two vectors are not in fixed proportion but instead vary with the inclination of  $k$ . A coordinate compression  $\xi \rightarrow \xi'$  that works for the coordinate compression  $k \rightarrow k'$  that works for the field (it expresses the change in dimensions of the convected through the shock) will not work for the noise field. An exception occurs when  $\xi''$  is chosen parallel to the shock plane (radial direction,  $x_1 = 0$ ). Then  $k'' = k$ , and since  $k'' = k$ , it follows that for this case  $k'' \cdot \xi'' = k \cdot \xi$ .

implies consideration of one

\* The local pressure field associated with turbulence, although weak by aerodynamic standards, may be strong by acoustic standards. If the turbulence (e. g., converted past a stationary microphone, a strong response can be observed; the phenomenon is called "pneudo-sound." The noise sensation produced by wind felt presumably a similar effect associated with turbulent separation of the flow.

\* A partial simplification is  $k'' \cdot \xi'' = k \cdot \xi$  if  $k'' = k$  and  $\xi'' = \xi$ .

of the coordinate axes, say  $x_i$ . In the former case,  $\underline{k} \cdot \underline{\xi}$  becomes  $k_i \xi_i$ ; and the exponential can be replaced by  $\cos k_i \xi_i$ , since the imaginary sine component will integrate out. Similarly  $e^{ik'' \cdot \underline{\xi}''}$  can be replaced by  $\cos k''_i \xi''_i$ .

**Cross-correlations.**—The phase angles of the transfer functions must be considered in formulating cross-correlations. For example, the correlation of local temperature with longitudinal velocity in the entropy and turbulence fields behind the shock is readily obtained as

$$\begin{aligned} \overline{\tau' u'}(0) &= \int (T e^{i\delta_T})^* (N e^{i\delta_s}) [u u] d\underline{k} \\ &= \int T N e^{i(\delta_s - \delta_T)} [u u] d\underline{k} \end{aligned}$$

The integrand, except for the exponential, is even in the wave inclination  $\theta$ ; the phase angles  $\delta_s$  and  $\delta_T$  (in the notation used) are odd in  $\theta$  (both properties can be inferred from the symmetry of the wave-refraction process with respect to  $\theta$ ). Accordingly, the imaginary sine term in the exponential will integrate out, and

$$\overline{\tau' u'}(0) = \int T N \cos(\delta_s - \delta_T) [u u] d\underline{k} \quad (40)$$

The corresponding relations for other cross-correlations can be written down by analogy.

#### CORRELATIONS BETWEEN TURBULENCE AND NOISE

Cross-correlations between the turbulence and noise fields require a special treatment, partly because of the inhomogeneity of the noise field, and partly because of the non-parallelism of the physically associated waves. In what follows, an expression for the correlation of noise pressure with longitudinal turbulent velocity will be derived. From this the qualitative variation of the correlation with distance downstream of the shock will be inferred.

The refracted shear wave ( $\sim \underline{k}'$ ) and pressure wave ( $\sim \underline{k}''$ ) associated in an elementary interaction process have different inclinations (fig. 3). As a consequence, the formal application of the relations given in the section **SPECTRAL ANALYSIS OF RANDOM FIELDS** leads to difficulty: the spectral density of any correlation appears to vanish according to equation (21). Actually, the formulas are inapplicable to correlations involving mutually inclined waves; this will be brought out clearly in the following derivation of the applicable formulas. For simplicity the derivation will be limited to the correlation of turbulent longitudinal velocity  $u'$  at point  $\underline{x}'$  with noise pressure  $p''$  at point  $\underline{x}''$ ; extensions to other cases are straightforward. The derivation will first be carried out as though the noise field were homogeneous (no variation of transfer function  $P$  with  $\underline{x}$ ), and then will be adapted to take account of the actual inhomogeneity.

The respective Fourier integrals may be written

$$u'(\underline{x}') = \int e^{ik' \cdot \underline{x}'} dZ_u(\underline{k}') = \int e^{-ik' \cdot \underline{x}'} dZ_u^*(\underline{k}')$$

$$p''(\underline{x}'') = \int e^{ik'' \cdot \underline{x}''} dZ_p(\underline{k}'')$$

The correlation may be formed as the ensemble average of the product  $u' p''$ :

$$\overline{u'(\underline{x}') p''(\underline{x}'')} = \int \int e^{ik' \cdot \underline{x}' - ik'' \cdot \underline{x}''} \overline{dZ_u^*(\underline{k}') dZ_p(\underline{k}'')} \quad (41)$$

where the bar has been taken inside the integral, since the operations of averaging and integration commute. Equation (7) and the first of equations (4) may be used to simplify the right side:

$$\overline{dZ_u^*(\underline{k}') dZ_p(\underline{k}'')} = N^*(\underline{k}') P(\underline{k}'') \overline{dZ_u^*(\underline{k}') dZ_u(\underline{k}'')} \quad (42)$$

where  $\underline{k}''$  bears the same relation to  $\underline{k}$  as  $\underline{k}''$  does to  $\underline{k}$ . By virtue of equation (20), equation (42) reduces further to

$$\overline{dZ_u^*(\underline{k}') dZ_p(\underline{k}'')} = N^*(\underline{k}') P(\underline{k}'') [u u] \delta(\underline{k}' - \underline{k}'') d\underline{k}' d\underline{k}''$$

if the fields are homogeneous. Substitution of this relation into equation (41) and integration over  $\underline{k}$  result in

$$\overline{u'(\underline{x}') p''(\underline{x}'')} = \int e^{ik' \cdot \underline{x}' - ik'' \cdot \underline{x}''} N^*(\underline{k}') P(\underline{k}'') [u u] d\underline{k} \quad (43)$$

since the  $\delta$ -function eliminates all values of  $\underline{k}'$  but  $\underline{k}$  and similarly all values of  $\underline{k}''$  but  $\underline{k}'$ . Finally, the equation may be generalized to apply to the actual inhomogeneous pressure field, according to equation (23) and the discussion preceding it, by writing  $P(\underline{k})$  as  $P(\underline{k}, x'_1)$  and using the value appropriate to  $x'_1$ .

Equation (43) is the general relation for the two-point correlation of longitudinal turbulent velocity  $u'$  with noise pressure  $p''$ . The striking feature is the difference of the exponential term from those in equations (13) and (22); this constitutes an a posteriori demonstration of the inapplicability of those equations.<sup>5</sup>

If the turbulent velocity and noise pressure are correlated locally ( $x'' = x'$ ), the expression simplifies to

$$\overline{u' p''(x')} = \int e^{i(k'_1 - k''_1)x'_1} N(\underline{k}) P(\underline{k}, x'_1) [u u] d\underline{k} \quad (44)$$

since  $k'_2 = k'_3$ ,  $k''_2 = k''_3$ . Directly at the shock,  $x'_1 = 0$  and the right side simplifies further; the integration can readily be carried out for isotropic turbulence, and a nonvanishing correlation will be obtained. Behind the shock ( $x'_1 > 0$ ), the exponential oscillates sinusoidally; for a given wave inclination the behavior is essentially like  $\cos C k x'_1$ , where  $C$  is a constant. For  $x'_1$  very small, the cosine is near unity over the significant range of  $k$  (the range for which  $[u u] \gg 0$ ). Hence the correlation is only slightly diminished at small distances behind the shock. At somewhat greater distances the oscillatory nature of the cosine begins to be felt before  $[u u]$  dies out, and the correlation falls off noticeably. Finally, at very large distances,  $\cos C k x'_1$  oscillates over a great

<sup>5</sup> However, eq. (43) is equivalent to that which would result from eq. (13) or (22) upon replacing the pressure wave by a locally equivalent shear wave parallel to the actual shear wave, as discussed in ref. 8.

many periods as  $k$  covers its important range, and the plus and minus contributions to the integral cancel each other; thus at these large distances behind the shock the noise-turbulence correlation falls to zero.

#### INTERACTION OF TURBULENCE WITH AN OBLIQUE SHOCK

All the foregoing analysis may be applied to an oblique shock by treating the latter as a normal shock with a superposed cross-velocity which is to be ignored. The coordinate system should be oriented so that the  $x_1$ -axis is normal to the oblique-shock front (on the downstream side), and the  $x_2$ - and  $x_3$ -axes lie in the shock front with the  $x_3$ -axis in the plane of the stream-velocity vector and the  $x_1$ -axis. The component of the stream velocity in the  $x_1$ -direction is the  $U$  velocity of the equivalent normal shock. From here on the analysis for the normal-shock case may be applied.

Ordinarily the turbulence spectrum tensor will be defined (as  $\Phi'_{ij}$ , say) in a system  $x'_1, x'_2, x'_3$  with the  $x'_1$ -axis aligned with stream direction, and it will be necessary to transform  $\Phi'_{ij}$  to the new system  $x_1, x_2, x_3$ . If the shock angle of the oblique shock is  $\psi$ , the primed and unprimed axes are related according to the following scheme:

$$\left. \begin{array}{ccc} & x_1 & x_2 & x_3 \\ \left. \begin{array}{l} x'_1 \\ x'_2 \\ x'_3 \end{array} \right\} & \begin{array}{l} r_{11} = \sin \psi \\ r_{21} = 0 \\ r_{31} = -\cos \psi \end{array} & \begin{array}{l} r_{12} = 0 \\ r_{22} = 1 \\ r_{32} = 0 \end{array} & \begin{array}{l} r_{13} = \cos \psi \\ r_{23} = 0 \\ r_{33} = \sin \psi \end{array} \end{array} \right\} \quad (45)$$

where  $r_{ij}$  is the cosine of the angle between  $x'_i$  and  $x_j$ . The transformation is effected by the formula

$$\Phi_{mn} = r_{im} r_{jn} \Phi'_{ij} \quad (46)$$

where the repeated indices  $i$  and  $j$  are to be summed over. The diagonal terms in the result are relatively simple:

$$\left. \begin{array}{l} \Phi_{11} = \Phi'_{11} \sin^2 \psi + \Phi'_{33} \cos^2 \psi - \sin \psi \cos \psi (\Phi'_{13} + \Phi'_{31}) \\ \Phi_{22} = \Phi'_{22} \\ \Phi_{33} = \Phi'_{11} \cos^2 \psi + \Phi'_{33} \sin^2 \psi + \sin \psi \cos \psi (\Phi'_{13} + \Phi'_{31}) \end{array} \right\} \quad (47)$$

The coordinate transformation whereby  $\Phi'_{ij}$  goes over into  $\Phi_{mn}$  may be illustrated most simply by choosing  $\Phi'_{ij}$  to correspond to isotropic turbulence; in that case,  $\Phi'_{ij}$  has the general form (e. g., ref. 12)

$$\Phi'_{ij} = F(k') (k'^2 \delta_{ij} - k'_i k'_j) \quad (48)$$

Substitution into the first of equations (47) yields

$$\begin{aligned} \Phi_{11} &= F(k') [(k'_2{}^2 + k'_3{}^2) \sin^2 \psi + (k'_2{}^2 + k'_1{}^2) \cos^2 \psi + 2k'_1 k'_3 \sin \psi \cos \psi] \\ &= F(k') [k'_2{}^2 + (k'_3 \sin \psi + k'_1 \cos \psi)^2] \end{aligned} \quad (49)$$

In the preceding equations,  $k'_1, k'_2, k'_3$  are the components of the wave-number vector in the primed coordinate system; these are related to the components  $k_1, k_2, k_3$  in the unprimed system precisely as  $x'_1, x'_2, x'_3$  are related to  $x_1, x_2, x_3$  in equations (45). As a consequence, equation (49) can be readily shown to reduce to

$$\Phi_{11} = F(k) [k_2^2 + k_3^2] \quad (50)$$

The corresponding element of equation (48) is

$$\Phi'_{11} = F(k') [k'_2{}^2 + k'_3{}^2] \quad (51)$$

Thus the tensor elements  $\Phi_{11}$  and  $\Phi'_{11}$  have the same functional form, reflecting the isotropic property of invariance under rotation of coordinates. This particular example of the coordinate rotation applied to isotropic turbulence is trivial in that the result could have been written down in advance without recourse to the transformation equation. Nevertheless, it illustrates the formal application of the transformation and, in addition, serves as a check on the first of equations (47) in yielding the required invariance.

#### CALCULATIONS

Numerical calculations have been carried out for flows in which the turbulence incident on the shock is (1) isotropic and (2) strongly axisymmetric. An account of the isotropic case follows. The more complicated axisymmetric case adds little of interest and is therefore left to appendix C.

#### MEAN-SQUARE VELOCITY COMPONENTS IN TURBULENCE FIELD

The equations that jointly relate the upstream (unprimed) and downstream (primed) mean squares are

$$\overline{u^2} = \int |uu| d\underline{k} \quad (52)$$

$$\overline{u'^2} = \int S^2 \frac{\cos^2 \theta'}{\cos^2 \theta} |uu| d\underline{k} \quad (53)$$

$$\overline{v'^2} - \overline{w'^2} = \int S^2 \frac{\sin^2 \theta' - \sin^2 \theta}{\cos^2 \theta} |uu| d\underline{k} + \overline{v^2} - \overline{w^2} \quad (54)$$

The first of these is just equation (14) with  $\alpha = u$ ; the last two result from substituting into equations (31) the expressions for  $|X|^2$  and  $|Y|^2$  from appendix A. So far the equations have not been specialized to isotropic initial turbulence.

When the initial turbulence is isotropic (i. e., has spherical symmetry), its longitudinal spectral density  $|uu|$  has the general form (e. g., ref. 12, eq. (3.4.12))

$$|uu| = k^2 F(k) \cos^2 \theta \quad (55)$$

where  $F(k)$  is an arbitrary function of  $k$ . ( $F(k)$  will ultimately cancel out in forming ratios.) It is appropriate, then, to go over to a form of spherical polar coordinates:

$$\left. \begin{array}{l} k_1 = -k \sin \theta \\ k_2 = k \cos \theta \cos \varphi \\ k_3 = k \cos \theta \sin \varphi \\ d\underline{k} = k^2 \cos \theta dk d\varphi d\theta \end{array} \right\} \quad (56)$$

Equations (52) and (53) may now be written

$$\overline{u^2} = 2 \int_0^\infty k^4 F(k) dk \int_0^{2\pi} d\varphi \int_0^{\pi/2} \cos^3 \theta d\theta \quad (57)$$

$$\overline{u'^2} = 2 \int_0^\infty k^4 F(k) dk \int_0^{2\pi} d\varphi \int_0^{\pi/2} |S|^2 \cos^2 \theta' \cos \theta d\theta \quad (58)$$

where the factor of 2 and the limit  $\pi/2$  result from the sym-

metry in  $\theta$ . Division of equation (58) by (57) yields, since  $\int_0^{\pi/2} \cos^3 \theta d\theta = \pi/3$ ,

$$\overline{u'^2}/\overline{u^2} = \frac{3}{2} \int_0^{\pi/2} S^2 \cos^2 \theta' \cos \theta d\theta \quad (59)$$

In a rather similar fashion, equation (36) yields

$$\overline{r'^2}/\overline{u^2} = \overline{w'^2}/\overline{u^2} = \frac{3}{4} \left( 1 + \int_0^{\pi/2} S^2 \sin^2 \theta' \cos \theta d\theta \right) \quad (60)$$

where use has been made of the initial isotropy  $\overline{u^2} = \overline{v^2} = \overline{w^2}$ , and final axisymmetry  $\overline{r'^2} = \overline{w'^2}$ .

The transfer function  $S$  in equations (59) and (60) is a measure of the amplification of a single spectral component in passing through the shock; the associated phase angle is  $\delta_s$  (not relevant here).  $S$ , like the other transfer functions, is a complicated function of  $\theta$  that does not lend itself to analytic integration. A numerical tabulation of  $S$  and  $\delta_s$  against  $\theta$  is given in tables I (c) to (k) for the respective Mach numbers of 1.10, 1.25, 1.5, 2.0, 2.5, 3.0, 4.0, 6.0, and  $\infty$ ; these tables were used in conjunction with numerical integration to evaluate equations (57) and (58). ( $S$  reduces to 1 for all  $\theta$  at  $M=1$ .)

#### MEAN-SQUARE TEMPERATURE IN ENTROPY FIELD

The derivation of  $\overline{r'^2}/\overline{u^2}$  is parallel to that of  $\overline{u'^2}/\overline{u^2}$ , equation (53) being replaced by equation (36). The result is (analog of eq. (59)):

$$\overline{r'^2} = \frac{3}{2} \overline{u^2} \int_0^{\pi/2} T^2 \cos^3 \theta d\theta \quad (61)$$

The transfer function  $T$  and the associated phase angle  $\delta_T$  (not relevant here) are tabulated against  $\theta$  in tables I (c) to (k) for the various Mach numbers. The tabulated values used in the numerical integration of equation (61).

#### MEAN-SQUARE PRESSURE IN NOISE FIELD

Because of the similarity of equations (34) and (36), the mean-square pressure can be written down by inspection of equation (61):

$$\overline{p'^2} = \frac{3}{2} \overline{u^2} \int_0^{\pi/2} P^2 \cos^3 \theta d\theta \quad (62)$$

The integration has been performed numerically with use of the definition of  $P$  in terms of  $\Pi$  (appendix A) and the values of  $\Pi$  against  $\theta$  tabulated in tables I (a) to (i), appropriate to  $x = \infty$ . Thus, the integral as evaluated refers to the asymptotic mean-square pressure far behind the shock.

### RESULTS AND DISCUSSION

The results of the calculations of the preceding section are shown in figure 4 for Mach numbers of 1 to  $\infty$ ; this figure evaluates the disturbance field—both turbulence and noise—downstream of a shock when isotropic turbulence is convected into the shock. The velocity perturbations, on a

root-mean-square basis, are in percent of stream velocity ahead of the shock (thus the basis is the same on both sides of the shock); the temperature and pressure perturbations are in percent of ambient behind the shock.<sup>6</sup> The velocity curves refer solely to the turbulence component, the temperature curve to the entropy component, and the pressure curve to the noise component of the field behind the shock.

The curves show that isotropic turbulence is somewhat transformed in passing through a shock, the longitudinal and lateral components no longer being equal; the selective effect is, however, mild compared with that of screens or wind-tunnel contractions (cf., e. g., ref. 14). In addition, although the incident flow was assumed isothermal and isotropic, the downstream flow possesses an entropy spottiness, which is a "frozen" convected pattern like the turbulence. The root-mean-square temperature associated with the entropy spottiness, in percent of ambient, is seen to be not much less than the root-mean-square velocity of the initial turbulence, in percent of free stream.

In the theory the entropy spottiness is spatially correlated with the longitudinal component of the turbulent velocity everywhere behind the shock. In practice it is to be expected that the correlation will soon be destroyed by eddy intermixing as the combined fields are convected downstream from the shock; this intermixing, being second order, is neglected in the linear theory. Directly at the shock, the noise pressure likewise is correlated with the longitudinal component of the turbulent velocity. According to the earlier qualitative examination, however, this correlation falls off with distance behind the shock, reaching zero far back.

The peculiar hump in the curve of root-mean-square noise pressure against Mach number just above  $M=1$  has commanded special attention. In order to delineate the shape accurately, additional numerical computations (beyond those for the other curves) were made at  $M=1.05$  and  $M=1.01$ . These were supplemented by an analytical study which established that the curve varies like  $(M-1)^{1/4}$  as  $M \rightarrow 1$ .

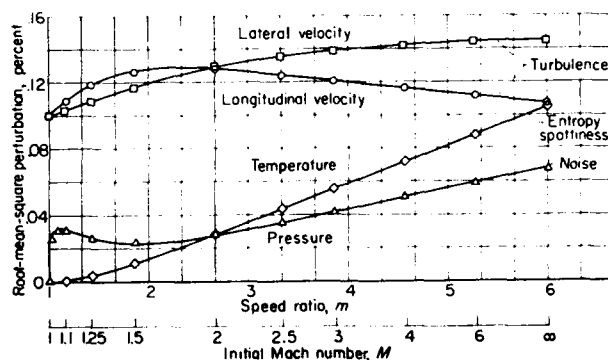


FIGURE 4. Disturbances produced behind shock by interaction with isotropic turbulence. Turbulent intensity just before shock, 0.1 percent. Root-mean-square velocity in percent of initial stream velocity ahead of shock; root-mean-square temperature and pressure in percent of ambient behind shock.

<sup>6</sup> For the circumstances of figs. 4 and 5, namely, longitudinal component of initial turbulence equals 0.1 percent of stream velocity, the dimensional quantities plotted are as follows in terms of the nondimensional symbols used in the analysis: longitudinal velocity, percent initial stream velocity,  $0.1 \sqrt{u'^2/u^2}$ ; lateral velocity, percent initial stream velocity,  $0.1 \sqrt{v'^2/u^2}$ ; temperature, percent ambient,  $0.1 \sqrt{m r'^2/u^2}$ ; pressure, percent ambient,  $0.1 \sqrt{m p'^2/u^2}$ .

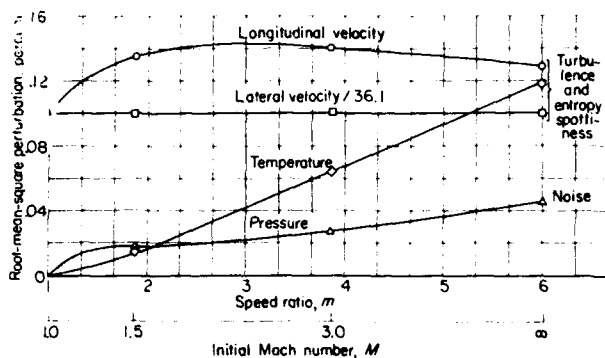


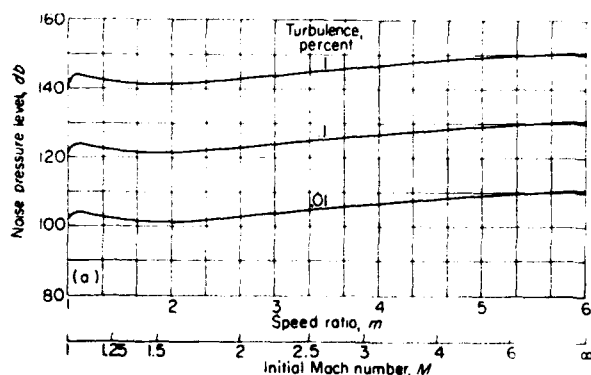
FIGURE 5.—Disturbances produced behind shock by interaction with strongly axisymmetric turbulence. Longitudinal intensity, 0.1 percent; lateral intensity is 3.61 percent just before shock. Root-mean-square velocity in percent of initial stream velocity; root-mean-square temperature and pressure in percent of ambient.

from above, approaching the limiting value of zero. The precise asymptotic expression is

$$0.1 \sqrt{\frac{m p'^{1/2}}{u^2}} = 0.1 \frac{\gamma}{\gamma+1} \left(\frac{8}{5}\right)^{1/2} 2^{1/4} (M-1)^{1/4} \quad (63)$$

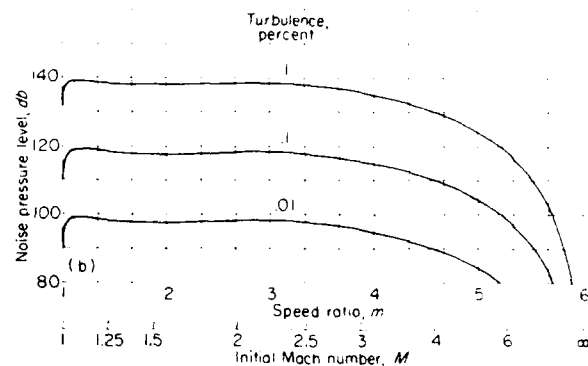
where the omitted next-higher-order term is  $O[(M-1)^{3/4}]$ .

Figure 4 applies when isotropic turbulence flows into the shock. Figure 5 (prepared from calculations described in appendix B) applies when strongly axisymmetric turbulence flows into the shock; the specifications for the turbulence were taken from theoretical calculations of the modifications in initially isotropic turbulence that had passed through damping screens and a wind-tunnel contraction (ref. 10, four screens,  $K=2$ ,  $M=1.5$ ). The calculated deviation from isotropy is based on idealized conditions and is probably an extreme upper limit to what might be encountered in a wind-tunnel test section. The longitudinal component of the incident turbulence is the same for both figures—namely, 0.1 percent of free-stream speed—but the lateral component is 3.61 percent for figure 5 against 0.1 percent (isotropic) for figure 4. Despite the wide disparity in the lateral component, however, comparison of the two figures shows no great change in the curves. Evidently, the lateral component of the turbulence flowing into the shock has little effect, and the



(a) Ambient pressure downstream of shock, 1 atmosphere.

FIGURE 6.—Noise generated by shock-turbulence interaction (isotropic turbulence).



(b) Stagnation pressure upstream of shock, 1 atmosphere.

FIGURE 6. (Concluded). Noise generated by shock-turbulence interaction (isotropic turbulence).

intensity of the remainder of the disturbance field behind the shock depends almost solely on the longitudinal component, regardless of the degree of anisotropy. The shock-induced change in the lateral component itself, however, depends on the deviation from isotropy, being appreciable for the isotropic case and quite negligible for the extreme axisymmetric case.

The noise generated by the shock-turbulence interaction is measured by the curves of root-mean-square pressure. This is best indicated by use of an acoustic scale as in figure 6. Here the noise pressure level is plotted in decibels above the standard reference base of 0.000204 microbar for several levels of initial isotropic turbulence. According to the preceding paragraph there would be little difference for strongly axisymmetric turbulence of the same longitudinal intensities; the difference between figures 4 and 5 corresponds to no more than 4 decibels at the Mach numbers (1.5, 3, and  $\infty$ ) for which there are comparable data.

The reference static pressure behind the shock is different for the two parts of figure 6. In figure 6(a) the ambient pressure behind the shock is constant with Mach number (1 atm); this situation may be approximated in an exit jet of an aircraft in flight. In figure 6(b) the stagnation pressure ahead of the shock is constant at 1 atmosphere, so that the static pressure behind the shock diminishes markedly with increasing Mach number; this situation is roughly characteristic of many wind-tunnel flows. It is seen that even at a longitudinal component of turbulence of 0.01 percent, the noise level is severe; and at 1 percent the noise level exceeds 130 decibels, which is of the order of the threshold of pain, over much of the Mach number range.

These remarks all refer to the asymptotic noise level an "infinite" distance behind the shock, since the attenuating part of the pressure waves has been neglected (in practice, this distance may be taken to be twice the longest significant wave length). For an initial Mach number of 1.5, the noise level is predicted to be some 17 decibels greater directly behind the shock where the attenuation is nil.

The local pressure level (proportional to the energy density) of the noise field in the region of shock-turbulence interaction is one aspect of the noise problem. Lighthill (ref. 3) has investigated another aspect, namely, the flux of acoustic energy radiated from the interaction region as a result of

the convection of any specified volume of turbulence through a weak plane shock segment ( $1 \leq M \leq 1.3$ ); the turbulence need not be homogeneous. The two quantities, energy density and flux of energy, are not simply related unless the wave pattern is simple, for example, parallel plane waves or concentric spherical waves.

### CONCLUDING REMARKS

The quantitative effects of the interaction of a convected homogeneous field of turbulence with an extended plane shock have been calculated, including the pressure level of the noise generated in the process. The assumed conditions are closely approximated in a supersonic wind tunnel or duct with a normal shock: the shock, together with its images in the walls (if the latter are nearly parallel), behaves substantially like an extended plane shock for the purposes of the analysis. The approximation is still quite good for plane oblique shocks for that portion of the incident turbulence whose eddies are small compared with the tunnel diameter

(spectral wave length  $\ll$  tunnel diam.), and probably fairly good even without this restriction on eddy size.

The propulsive free jet emitted by a turbojet, ram-jet, or rocket engine is turbulent, but the turbulence is far from homogeneous. In addition, only local segments of the shock structure that may occur aft of the nozzle can be considered sensibly plane. The shock-interaction noise generated by turbulent eddies smaller than such shock segments can perhaps be estimated from the curves presented herein. Estimates of this sort refer to the sound pressure level within the jet and nearby outside; they provide no direct information on the sound pressure level far from the jet as a function of distance and direction, or on the total acoustic power radiated by the jet.

LEWIS FLIGHT PROPULSION LABORATORY

NATIONAL ADVISORY COMMITTEE FOR AERONAUTICS

CLEVELAND, OHIO, June 3, 1954

## APPENDIX A

### SYMBOLS

The following symbols are used in this report: (In appendix B some alternate symbols are defined and used in certain parts.)

$a$	function defined in ref. 2
$a^*$	critical speed of sound
$b$	function defined in ref. 2
$F(k)$	arbitrary function of $k$
$G(\theta)$	screen-effect function, $G(\theta) = \frac{4\alpha^2 \sin^2 \theta + \nu^2 \cos^2 \theta}{4 \sin^2 \theta + \mu^2 \cos^2 \theta}$
$H(\theta)$	contraction-effect function, $H(\theta) = \frac{l_2^2}{l_1} \frac{1}{(\epsilon \sin^2 \theta + \cos^2 \theta)^2}$
$J'$	Jacobian of transformation from $k$ to $\underline{k}'$ , $J' = \frac{dk}{dk'} = \frac{1}{m}$
$J''$	Jacobian of transformation from $\underline{k}$ to $\underline{k}''$ , $J'' = \frac{d\underline{k}}{d\underline{k}''} = \frac{\cos^2 \theta''}{m \cos^2 \theta'} \frac{\partial \theta'}{\partial \theta''}$
$K$	screen coefficient, $K = \frac{\text{pressure drop}}{\text{dynamic pressure}}$
$k$	amplitude of $\underline{k}$ : $k^2 = k_1^2 + k_2^2 + k_3^2 = k_1^2 + k_r^2$
$k_r$	radial component of $\underline{k}$ , $k_r = -k_1 \cot \theta$
$\underline{k}$	wave-number vector, $\underline{k} = k_1, k_2, k_3$ ; also, $\underline{k} = k_1, k_r, 0$ in cylindrical coordinates
$d\underline{k}$	volume element in wave-number space, $d\underline{k} = dk_1 dk_2 dk_3$
$l_1$	contraction parameter, $l_1 = \frac{\text{final stream speed}}{\text{initial stream speed}}$
$l_2$	contraction parameter, $l_2 = \frac{\text{final stream-tube width}}{\text{initial stream-tube width}}$
$M$	Mach number upstream of normal shock
$M_1$	Mach number downstream of normal shock

$m$	ratio of speeds before and after shock, $m = \frac{(\gamma+1)M^2}{2+(\gamma-1)M^2}$
$N$	number of damping screens
$P$	transfer function for sound waves (pressure effect), $P = \frac{-2\gamma \sqrt{m} \Pi \sec \theta \sec \theta'}{(\gamma+1)m - (\gamma-1)}$
$p$	pressure perturbation
$p$	mean static pressure
$R_{ij}(\xi)$	perturbation velocity correlation tensor (special case of $\alpha\beta(\xi)$ )
$r_i$	direction cosines
$S$	transfer function for shear waves, tabulated in tables I(c) to (k) (eq. in ref. 2)
$T$	$\frac{2(\gamma-1)(m-1)^2}{\sqrt{m} [(\gamma+1)m - (\gamma-1)]} \sqrt{(a \tan \theta - 1)^2 + (b \tan \theta)^2}$ , $0 \leq \theta \leq \frac{\pi}{2}$
$\mathcal{T}$	Transfer function for entropy waves (temperature effect) $\mathcal{T} = T e^{i\delta} T$
$U$	stream velocity downstream of shock
$U_A$	stream velocity upstream of shock
$u, v, w$	nondimensional disturbance velocity components in directions $x_1, x_2, x_3$ , respectively; $u, v, w = \frac{\text{components of velocity perturbation}}{\text{critical speed of sound } a^*}$
$V$	cross-stream velocity (sketch (c))
$v_r$	disturbance velocity component in radial direction/ $a^*$
$v_\varphi$	disturbance velocity component in $\varphi$ -direction/ $a^*$
$W$	resultant of $U$ and $V$
$dW_\theta$	(complex) wave amplitude in two-dimensional field



$X$	transfer function, $X = Se^{i\theta_s} \frac{\cos \theta'}{\cos \theta}$	$\theta_{cr}$	critical value of $\theta$ for which $W =$ speed of sound
$\underline{x}$	position vector, $\underline{x} = x_1 = x_2, x_3$	$\underline{\kappa}$	wave-number vector, $\underline{\kappa} = \kappa_1, \kappa_2, \kappa_3$
$Y$	transfer function, $Y = Se^{i\theta_s} \frac{\sin \theta'}{\sin \theta}$	$\mu$	screen parameter, $\mu = 1 + \alpha_s + K$
$dZ_r$	(complex) wave amplitude associated with $r$	$\nu$	screen parameter, $\nu = 1 + \alpha_s + \alpha_s K$
$dZ_u$	(complex) wave amplitude associated with $\alpha$	$\xi$	separation of two points, $\xi = \hat{x} - \hat{x}$
$dZ_\varphi$	(complex) wave amplitude associated with $\varphi$	$\Pi$	function tabulated in table I (defined in ref. 2)
$\alpha, \beta$	may stand for $u, v, w, p, \rho$ , or $\tau$	$\Pi$	transfer function for sound waves, $\Pi = \Pi e^{i\theta_s}$
$\alpha_s$	screen parameter, $\alpha_s^2 = \frac{1.21}{1+K}$ for $K \geq 1$	$\rho$	density perturbation
$\overline{\alpha\beta}(\xi)$	correlation of $\alpha$ and $\beta$ at a separation $\xi$	$\bar{\rho}$	mean density
$[\alpha\beta](\underline{k})$	Fourier transform of $\overline{\alpha\beta}(\xi)$ , interpreted as spectral density of $\overline{\alpha\beta}(0)$	$\tau$	temperature perturbation
$\beta_u$	$\beta_u = \frac{M_1^2}{\cos^2 \theta'} - 1$	$T$	mean temperature
$\Gamma_{ij}(\underline{k})$	perturbation velocity spectrum tensor (special case of $[\alpha\beta](\underline{k})$ )	$\Phi_{ij}(\underline{k})$	perturbation velocity spectrum tensor (special case of $[\alpha\beta](\underline{k})$ )
$\gamma$	ratio of specific heats (taken as 1.4)	$\varphi$	common longitude angle of wave normals $\underline{\kappa}, \underline{k}, \underline{k}', \underline{k}''$ in polar coordinates
$\delta_p$	phase angle of $\Pi$ (eq. in ref. 2)	$\chi$	transfer function, $\chi = \Pi \left( \frac{\cos \theta' - e^{i\pi/2} \beta_u \sin \theta'}{\cos \theta} \right)$
$\delta_s$	phase angle of $X$ and $Y$ , tabulated in tables I(c) to (k) (eq. in ref. 2)	$\Upsilon$	transfer function, $\Upsilon = \Pi \left( \frac{\sin \theta' - e^{i\pi/2} \beta_u \cos \theta'}{\sin \theta} \right)$
$\delta_T$	phase angle of $\underline{T}$ , tabulated in tables I(c) to (k), $\delta_T = \tan^{-1} \left( \frac{b}{\cot \theta - a} \right), 0 \leq \theta \leq \frac{\pi}{2}$	where	
$\epsilon$	contraction parameter, $\epsilon = F_2^2 / F_1^2$	$u = 1, 0 \leq \theta \leq \theta_{cr}$	
$\theta$	shear-wave inclination ahead of contraction, $\theta = \tan^{-1} \left( \frac{l_1}{l_2} \tan \theta \right)$	$\theta = 0, \theta_{cr} \leq \theta \leq \frac{\pi}{2}$	
$\theta'$	shear-wave inclination behind shock (see fig. 3), $\theta' = \tan^{-1}(m \tan \theta)$	$\psi$	acute angle between oblique shock and upstream flow direction
$\theta''$	sound-wave inclination behind shock (see fig. 3), $\theta'' = \begin{cases} -\tan^{-1} \frac{M^2 \tan \theta}{1-M^2}, & 0 \leq \theta \leq \theta_{cr} \\ \theta' - \cot^{-1} \beta_u, & \theta_{cr} \leq \theta \leq \frac{\pi}{2} \end{cases}$	Subscripts:	
		$\alpha, \beta$	may stand for $u, v, w, p, \rho$ , or $\tau$
		$i, j, m, n$	may stand for 1, 2, or 3; used to replace $\alpha$ and $\beta$ when $u, v, w$ are replaced by $u_1, u_2, u_3$ , respectively
		Superscripts:	
		$*$	complex conjugate
		$'$	refracted shear-entropy wave
		$''$	sound wave
		$\wedge$	distinguishing mark

## APPENDIX B

### COMPLETE VELOCITY SPECTRUM TENSORS

The first and the sum of the second and third diagonal terms of the spectrum tensors of the velocity field behind the shock are obtained in the text by use of a simplified approach. Other terms are occasionally of interest; for example, the separate values of the second and third diagonal terms are needed for a description of anisotropic turbulence. The complete spectrum tensor for each field (turbulence and noise) will be derived herein by a more comprehensive procedure.

**Turbulence field.** It will be convenient to replace the symbols  $u, v, w$  by  $u_1, u_2, u_3$ , and to replace  $\alpha$  and  $\beta$  by  $i, j$ , which take on the values 1, 2, and 3 instead of  $u, v$ , and  $w$ . With this notation and the use of equations (8), equations (10) can be transformed to

$$dZ'_1 = X dZ_1$$

$$dZ'_2 = (Y-1)dZ_r \cos \varphi + dZ_2$$

$$dZ'_3 = (Y-1)dZ_r \sin \varphi + dZ_3$$

By introduction of the geometric relations (figs. 1 and 2)

$$\left. \begin{aligned} dZ_r &= dZ_1 \tan \theta \\ \tan \theta &= -k_1/k_r \\ \cos \varphi &= -k_2/k_r \\ \sin \varphi &= -k_3/k_r \end{aligned} \right\} \quad (B1)$$

all three equations may be represented by the single expression

$$dZ'_i = X dZ_1 \delta_{ii} + \left[ (Y-1) \left( -\frac{k_1 k_o}{k_r^2} \right) dZ_1 + dZ_i \right] (1 - \delta_{ii}) \quad (B2)$$

where

$$\delta_{ij} = \begin{cases} 1, & i=j \\ 0, & i \neq j \end{cases}$$

Multiplication of the complex conjugate of equation (B2) by the corresponding equation with subscript  $j$  and by  $k_j^4$  yields, after averaging,

$$\begin{aligned} k_j^4 \overline{dZ_j^* dZ_j} = & k_j^4 X^{-2} \overline{dZ_j^{-2}} \delta_{ij} + (1 - \delta_{ij})(1 - \delta_{ii}) \times \\ & [k_1^2 k_i k_j Y - 1^{-2} \overline{dZ_1^{-2}} + k_1^4 \overline{dZ_1^* dZ_j}] + \\ & k_1 k_i k_j^2 (1 - Y^*) \overline{dZ_1^* dZ_j} + k_i k_j k_j^2 (1 - Y) \overline{dZ_j dZ_1^*} + \\ & \delta_{ii}(1 - \delta_{ii}) X^* [k_1 k_j k_j^2 (1 - Y) \overline{dZ_1^{-2}} + k_1^4 \overline{dZ_1^* dZ_j}] + \\ & \delta_{ii}(1 - \delta_{ii}) X [k_1 k_i k_j^2 (1 - Y^*) \overline{dZ_1^{-2}} + k_1^4 \overline{dZ_1^* dZ_j^*}] \quad (B3) \end{aligned}$$

Now, if in equation (15) the symbol for the spectral tensor is changed from  $\alpha\beta$  to the more conventional symbol  $\Phi_{ij}$ , application to equation (B3) yields

$$\begin{aligned} \Phi_{ij} d\underline{k}' = & \left\{ \frac{dk_j}{k_j^4} k_j^4 X^{-2} \Phi_{ii} \delta_{ij} + (1 - \delta_{ii})(1 - \delta_{ii}) [k_1^2 k_i k_j Y - 1^{-2} \Phi_{ii} + \right. \\ & k_1^4 \Phi_{ii} + k_1 k_i k_j^2 (1 - Y^*) \Phi_{ij} + k_i k_j k_j^2 (1 - Y) \Phi_{ji} + \\ & \delta_{ii}(1 - \delta_{ii}) X^* [k_1 k_j k_j^2 (1 - Y) \Phi_{ii} + k_1^4 \Phi_{ii}] + \\ & \left. \delta_{ii}(1 - \delta_{ii}) X [k_1 k_i k_j^2 (1 - Y^*) \Phi_{ii} + k_1^4 \Phi_{ii}] \right\} \quad (B4) \end{aligned}$$

The elements of the turbulence spectrum tensor  $\Phi_{ij}$  may be exhibited in expanded matrix form:

$$\begin{aligned} k_j^4 X^{-2} \Phi_{ii} = & X^* [k_1 k_j k_j^2 (1 - Y) \Phi_{ii} + X^* [k_1 k_j k_j^2 (1 - Y) \Phi_{ii} + \\ & k_j^4 \Phi_{ii}] \\ k_j^4 \Phi_{22} = & k_j^4 \Phi_{22} + \\ & k_1^4 k_j^2 Y - 1^{-2} \Phi_{ii} + k_1^2 k_j k_j Y - 1^{-2} \Phi_{ii} + \\ & k_1 k_j k_j^2 (1 - Y^*) \Phi_{ii} + k_1 k_j k_j^2 (1 - Y^*) \Phi_{ii} + \\ & k_1 k_j k_j^2 (1 - Y) \Phi_{ii}^* \\ k_j^4 \Phi_{33} = & k_j^4 \Phi_{33} + k_1^4 k_j^2 Y - 1^{-2} \Phi_{ii} + \\ & k_1 k_j k_j^2 (1 - Y^*) \Phi_{ii} + \\ & k_1 k_j k_j^2 (1 - Y) \Phi_{ii}^* \end{aligned}$$

The matrix is Hermitian; that is, the missing elements are

the complex conjugates of the respective elements diagonally opposite; that is,  $\Phi_{11}^* = \Phi_{11}$ , and so forth.

It can be shown, by use of the continuity relation  $k_j \Phi_{ij} = 0$  (summed over repeated index), that after some reduction

$$(\Phi_{22}^* - \Phi_{33}^*) d\underline{k}' = \left[ (Y^{-2} - 1) \Phi_{ii} \frac{k_1^2}{k_j^2} + \Phi_{22} + \Phi_{33} \right] d\underline{k}$$

in agreement with the second of equations (29).

**Noise field.** With use of equations (B1), the three equations (11) may be represented by the single expression

$$dZ_j'' = \chi dZ_i \delta_{ij} - \Upsilon \left( \frac{k_1 k_i}{k_j^2} \right) dZ_i (1 - \delta_{ii}) \quad (B5)$$

where again the subscripts 1, 2, 3 replace  $u, v, w$ , and  $\delta_{ii} = 0$  or 1 as before. Starting with this equation, the spectral tensor  $\Phi_{ij}''$  may be derived in a straightforward manner by a procedure parallel to that leading from equation (B2) to (B4). The result is

$$\begin{aligned} \Phi_{ij}'' d\underline{k}'' = & \Phi_{ii} d\underline{k} \left\{ \chi^{-2} \delta_{ij} \delta_{ii} + \Upsilon^{-2} \frac{k_1^2 k_i k_j}{k_j^4} (1 - \delta_{ii})(1 - \delta_{ii}) \right. \\ & \left. \frac{k_1}{k_j^2} \chi - \Upsilon [\delta_{ii}(1 - \delta_{ii}) k_j + \delta_{ii}(1 - \delta_{ii}) k_i] \right\} \quad (B6) \end{aligned}$$

(The valid range of this equation has been limited to  $\theta_{cr} \leq \theta \leq \frac{\pi}{2} \left( \frac{k_1}{k_j} \geq \tan \theta_{cr} \right)$  by use of the simplification  $\chi \Upsilon^* = \chi^* \Upsilon = \chi - \Upsilon$ , which fails outside that range.)

The expanded form of equation (B6) is

$$\begin{aligned} \Phi_{ij}'' d\underline{k}'' = & \Phi_{ii} \frac{dk_j}{k_j^4} \left[ \chi^{-2} k_j^4 \right. \\ & - \chi \Upsilon k_1 k_2 k_j^2 - \chi \Upsilon k_1 k_3 k_j^2 \\ & - \chi \Upsilon k_1 k_3 k_j^2 - \Upsilon^{-2} k_1^2 k_j^2 \\ & - \Upsilon^{-2} k_1^2 k_j^2 - \Upsilon^{-2} k_1^2 k_j^2 \\ & - \Upsilon^{-2} k_1^2 k_j^2 - \Upsilon^{-2} k_1^2 k_j^2 \left. \right] \end{aligned}$$

The diagonal terms yield

$$\begin{aligned} \Phi_{ii}'' d\underline{k}'' = & \chi^{-2} \Phi_{ii} d\underline{k} \\ (\Phi_{22}'' - \Phi_{33}'') d\underline{k}'' = & \Upsilon^{-2} \frac{k_1^2}{k_j^2} \Phi_{ii} d\underline{k} \end{aligned}$$

since  $k_2^2 + k_3^2 = k_j^2$ ; these are in agreement with equations (30).

## APPENDIX C

### CALCULATIONS FOR AXISYMMETRIC INITIAL TURBULENCE

If the turbulence in the settling chamber of a supersonic wind tunnel is considered to be isotropic, by the time it reaches the working section it will be axisymmetric, with the longitudinal velocity perturbations very much less than the lateral perturbations; the change is due to the effects of the damping screens and the contraction (refs. 9, 13, and 14). The shock-interaction behavior for a particular case of extreme axisymmetry will be calculated herein as a matter of interest.

According to reference 14 (with a slight change in notation), if the longitudinal spectral density in the settling chamber (station  $A'$ ) is written as

$$[uu]_0 = \kappa^2 F(\kappa) \cos^2 \Theta \quad (\text{isotropic turbulence})$$

then the longitudinal density in the working section (station  $A$ ) is given by

$$[uu] = \kappa^2 F(\kappa) \cos^2 \Theta G^N(\Theta) H(\Theta) \quad (\text{axisymmetric turbulence}) \quad (C1)$$

where  $\kappa$  is the wave number at  $A'$ ,  $\Theta$  is the associated wave inclination,  $N$  is the number of damping screens,  $G(\Theta)$  depends on the screen pressure-drop coefficient  $K$ , and  $H(\Theta)$  depends on the parameters  $l_1$  and  $l_2$  defining the wind-tunnel

contraction. (See appendix A for the functional forms.) In what follows,  $N=4$ ,  $K=2$ ,  $l_1=24.92$ , and  $l_2=0.3186$ .<sup>7</sup> This set of values corresponds (in theory) to an axisymmetric turbulence at station A (just upstream of the shock) such that the root-mean-square lateral velocity component is 36.1 times the root-mean-square longitudinal component (see table I, p. 46, ref. 14). The ratio 36.1:1 is clearly an extreme deviation from isotropy.

The effects of the changed form of  $[uu]$  on the integration procedure will be illustrated by considering the mean-square longitudinal velocity in the turbulence. The relevant question is (53), with  $[uu]$  being given by equation (C1). From the form of equation (C1) it will be convenient to carry out the integrations in terms of  $\underline{k}$ , rather than  $\underline{k}$ ; the transformation is

$$d\underline{k} = \frac{1}{l_1 l_2^2} d\underline{k} = \frac{1}{l_1 l_2^2} \kappa^2 d\kappa d\varphi \cos \Theta d\Theta$$

Equation (35) then assumes the form

$$\overline{u'^2} = \frac{2}{l_1 l_2^2} \int_0^{\pi/2} S^2 \frac{\cos^2 \theta'}{\cos^2 \theta} G^N H \cos^3 \Theta d\Theta \int_0^\infty \kappa^4 G(\kappa) d\kappa \int_0^{2\pi} d\varphi$$

The last two integrals appear in the expression for  $\overline{u_0^2}$ , the mean-square longitudinal velocity at station A' (the expression is of the form of eq. (57)); thus, equation (C2) may be simplified to

$$\frac{\overline{u'^2}}{\overline{u_0^2}} = \left( \frac{3/2}{l_1 l_2^2} \right) \int_0^{\pi/2} S^2 \frac{\cos^2 \theta'}{\cos^2 \theta} G^N H \cos^3 \Theta d\Theta \quad (C3)$$

The variable of integration may be changed from  $\Theta$  to  $\theta$  by means of the transformation

$$d\Theta = \frac{1}{\sqrt{\epsilon}} \frac{\cos^2 \theta}{\cos^2 \theta'} d\theta$$

This results in the alternate form

$$\frac{\overline{u'^2}}{\overline{u_0^2}} = \left( \frac{3/2}{l_1 l_2^2} \right) \int_0^{\pi/2} S^2 \frac{\cos^2 \theta'}{\cos^2 \theta} G^N H \frac{\cos^2 \Theta \cos^3 \Theta d\Theta}{\sqrt{\epsilon}} \quad (C4)$$

On numerical evaluation, the integrand of equation (C3) was found to have a sharp peak near the upper limit, and

that of (C4) a sharp peak at the origin. The peaks were avoided by dividing the range of numerical integration among the two equations: (C3) was used over the range  $0 < \Theta < \Theta_1$  and (C4) was used over the range  $5^\circ < \theta < 90^\circ$ , where  $\Theta_1$  is the value of  $\Theta$  corresponding to  $\theta = 5^\circ$ .

## REFERENCES

1. Lighthill, M. J.: On Sound Generated Aerodynamically. I. General Theory. *Proc. Roy. Soc. (London)*, ser. A, vol. 211, no. 1107, Mar. 20, 1952, pp. 564-587.
2. Ribner, H. S.: Convection of a Pattern of Vorticity Through a Shock Wave. *NACA Rep.* 1164, 1954. (Supersedes NACA TN 2864.)
3. Lighthill, M. J.: On the Energy Scattered from the Interaction of Turbulence with Sound or Shock Waves. *Proc. Cambridge Phil. Soc.*, vol. 49, pt. 3, July 1953, pp. 531-551.
4. Moore, Franklin K.: Unsteady Oblique Interaction of a Shock Wave with a Plane Disturbance. *NACA Rep.* 1165, 1954. (Supersedes NACA TN 2879.)
5. Kováznay, Leslie S. G.: Turbulence in Supersonic Flow. *Jour. Aero. Sci.*, vol. 20, no. 10, Oct. 1953, pp. 657-674; 682.
6. Chang, C. T.: On the Interaction Between Weak Fluctuating Fields of Sound, Vorticity, and Temperature with an Oscillating Shock. Pt. I—In an Infinitely Extended Medium. *Dept. Aero., The Johns Hopkins Univ.*, Dec. 1, 1953. (Contract N6ori-105, Task Order III.)
7. Moore, Franklin K.: Passage of Flow Disturbances Through a Duct Containing Screens, Shocks, or Contractions. *Proc. Third Midwestern Conf. on Fluid Mech.*, Univ. of Minn., 1953, pp. 193-216.
8. Ribner, H. S., and Moore, F. K.: Unsteady Interaction of Disturbances with a Shock Wave, with Applications to Turbulence and Noise. *Heat Transfer and Fluid Mech. Inst.*, Stanford Univ. Press, 1953, pp. 45-55.
9. Ribner, H. S., and Tucker, M.: Spectrum of Turbulence in a Contracting Stream. *NACA Rep.* 1113, 1953. (Supersedes NACA TN 2606.)
10. Moyal, J. E.: The Spectra of Turbulence in a Compressible Fluid: Eddy Turbulence and Random Noise. *Proc. Cambridge Phil. Soc.*, vol. 48, pt. 2, Apr. 1952, pp. 329-344.
11. James, Hubert M., Nickols, Nathaniel B., and Phillips, Ralph S., eds.: *Theory of Servomechanisms*. First ed., McGraw-Hill Book Co., Inc., 1947, pp. 262-308.
12. Batchelor, G. K.: *The Theory of Homogeneous Turbulence*. Cambridge Univ. Press, 1953.
13. Taylor, G. I., and Batchelor, G. K.: The Effect of Wire Gauze on Small Disturbances in a Uniform Stream. *Quart. Jour. Mech. Appl. Math.*, vol. II, 1949, pp. 1-29.
14. Tucker, Maurice: Combined Effect of Damping Screens and Stream Convergence on Turbulence. *NACA TN* 2878, 1953.

<sup>7</sup> The values of  $l_1$  and  $l_2$  correspond to Mach numbers of 0.05 and 1.5 at stations A' and A, respectively. In the calculations, however, these same values of  $l_1$  and  $l_2$  will be maintained even though the Mach number at A is varied, in order to maintain the turbulent spectrum unchanged.

TABLE I.—WAVE ANGLES AND TRANSFER FUNCTIONS

(a) $M=1.01$ ( $m=1.01699$ ) (abbreviated table)				(c) $M=1.10$ ( $m=1.16908$ )							
$\theta_s$ , deg	$\theta'_s$ , deg	$\theta''_s$ , deg	$\Pi$	$\theta$ , deg	$\theta'$ , deg	$\theta''$ , deg	$S$	$\Pi$	$T$	$\delta_s$ , deg	$\delta_r$ , deg
7.92542( $\theta_{cr}$ )	8.056	-81.944	1.6345	0	0	0	1.145	-0.6667	-0.008792	0	180.00
7.95000	8.061	-81.261	1.3923	5	5.84	-26.75	1.145	-0.6508	-0.007888	49	156.00
7.97500	8.106	-80.968	1.3017	10	11.65	-45.45	1.148	-0.6048	-0.007777	90	129.76
8.00000	8.132	-80.757	1.2363	15	17.39	-57.07	1.152	-0.5318	-0.007767	141	97.30
8.25000	8.386	-79.278	.9132	18	20.80	-61.89	1.157	-0.4779	-0.007750	161	70.12
8.43785	8.577	-78.471	.7870	20	23.05	-64.51	1.161	-0.4362	-0.007800	70	41.90
8.95028	9.067	-76.662	.5826	20.268	23.35	-64.83	1.161	-0.4339	-0.007883	62	36.37
9.46271	9.618	-75.111	.4655	20.536	23.65	-65.14	1.162	-0.4290	-0.007886	51	26.73
9.97514	10.138	-73.685	.3824	20.804	23.95	-65.45	1.162	-0.4233	-0.007889	37	21.07
10.48757	10.659	-72.339	.3232	21.072( $\theta_{cr}$ )	24.25	-65.75	1.163	-0.4179	-0.007891	0	0
11.0	11.179	-71.045	.2778	21.100	24.28	-64.45	1.161	-0.2582	-0.007808		
12.5	12.702	-67.445	.1902	21.400	24.62	-61.02	1.155	.9378	-0.05845		
14	14.224	-64.014	.1383	21.800	25.06	-58.41	1.152	.7620	-0.04779		
15	15.239	-61.783	.1142	22.200	25.50	-56.34	1.149	.6511	-0.04111		
20	20.307	-50.990	.0598	22.500	25.90	-54.69	1.147	.5769	-0.03663		
25	25.365	-40.502	.0251	24.048	27.55	-48.95	1.141	.2856	-0.02511		
30	30.412	-30.164	.0124	25.536	29.18	-44.07	1.135	.2778	-0.01860		
35	35.447	-19.916	.0057	27.021	30.81	-39.50	1.130	.2696	-0.01428		
40	40.468	-9.739	.0019	28.512	32.42	-35.38	1.125	.1561	-0.01037		
45	45.474	.384	-.0001	30	34.02	-31.36	1.121	.1187	-0.00873		
50	50.466	10.460	-.0011	35	39.30	-18.76	1.105	.0448	-0.00373		
55	55.444	20.495	-.0014	40	44.45	-7.08	1.080	.0105	-0.00101		
60	60.409	30.493	-.0014	45	49.46	3.98	1.075	-.0057	-0.00066		
65	65.361	40.461	-.0012	50	54.33	14.58	1.060	-.0125	-0.00176		
70	70.303	50.401	-.0008	55	59.08	24.78	1.047	-.0141	-0.00252		
75	75.235	60.320	-.0005	60	63.72	34.66	1.035	-.0129	-0.00307		
80	80.161	70.223	-.0002	65	68.26	44.28	1.025	-.0103	-0.00346		
85	85.082	80.114	-.0001	70	72.71	53.68	1.016	-.0072	-0.00371		
90	90	90		75	77.06	62.91	1.009	-.0043	-0.00385		
				80	81.42	72.01	1.004	-.0020	-0.00398		
				85	85.72	81.02	1.001	-.0005	-0.00416		
				90	90	90	0				

(b) $M=1.05$ ( $m=1.08308$ ) (abbreviated table)				(d) $M=1.25$ ( $m=1.42857$ )							
$\theta_s$ , deg	$\theta'_s$ , deg	$\theta''_s$ , deg	$\Pi$	$\theta$ , deg	$\theta'$ , deg	$\theta''$ , deg	$S$	$\Pi$	$T$	$\delta_s$ , deg	$\delta_r$ , deg
16.3223( $\theta_{cr}$ )	17.61	-72.39	1.5246	0	0	0	1.300	-0.6667	-0.04059	0	180.00
16.400	17.69	-70.59	1.2371	5	7.12	-13.66	1.302	-0.6453	-0.04051	1.57	163.64
16.680	17.94	-68.59	.9905	10	14.14	-26.09	1.307	-0.5840	-0.04040	2.98	146.17
16.936	18.27	-66.81	.8375	15	20.95	-36.66	1.317	-0.4882	-0.04018	4.04	125.99
17.240	18.59	-65.35	.7307	20	27.47	-45.31	1.335	-0.3684	-0.03998	4.47	99.65
17.549	18.92	-64.05	.6499	23	31.23	-49.70	1.353	-0.2926	-0.04000	4.11	76.76
18.162	19.58	-61.74	.5336	25	33.67	-52.33	1.371	-0.2466	-0.04019	3.22	53.49
18.775	20.23	-59.66	.4508	26	34.87	-53.57	1.383	-0.2229	-0.04039	2.20	34.30
19.388	20.88	-57.72	.3876	28.300	35.22	-53.93	1.387	-0.2172	-0.04048	1.67	25.44
20.001	21.52	-55.88	.3377	28.656( $\theta_{cr}$ )	35.65	-54.35	1.392	-0.2106	-0.04059	0	0
25	26.82	-42.64	.1357	26.742	35.75	-51.36	1.373	.969	-0.03261		
30	32.04	-30.75	.0611	26.828	35.85	-50.07	1.366	.884	-0.02880		
35	37.20	-19.49	.0257	26.914	35.95	-49.05	1.360	.822	-0.02774		
40	42.29	-8.52	.0076	27	36.05	-48.15	1.356	.773	-0.02613		
45	47.31	1.96	-.0016	27.5	36.64	-44.27	1.338	.593	-0.02029		
50	52.26	12.30	-.0058	28	37.22	-41.28	1.326	.484	-0.01880		
55	57.14	22.44	-.0071	29	38.38	-36.35	1.307	.3484	-0.01257		
60	61.96	32.41	-.0067	30	39.52	-32.16	1.283	.2614	-0.00553		
65	66.72	42.23	-.0055	35	45.01	-15.45	1.238	.0658	-0.00276		
70	71.44	51.93	-.0039	40	50.16	-1.86	1.195	-.0007	-0.00004		
75	76.12	61.53	-.0024	45	55.01	10.13	1.157	-.0261	-0.00157		
80	80.76	71.06	-.0011	50	59.57	21.02	1.123	-.0337	-0.00252		
85	85.39	80.54	-.0003	55	63.89	31.10	1.094	-.0327	-0.00316		
90	90	90		60	67.99	40.54	1.068	-.0277	-0.00360		
				65	71.92	49.48	1.047	-.0211	-0.00392		
				70	75.71	58.02	1.030	-.0143	-0.00414		
				75	79.38	66.27	1.017	-.0084	-0.00430		
				80	82.96	74.29	1.008	-.0038	-0.00440		
				85	86.50	82.18	1.002	-.0010	-0.00446		
				90	90	90					

\*These values apply for  $r=0$  only. For  $r=\infty$ , values should be replaced by 0. All other values are independent of  $r$ .

TABLE I. WAVE ANGLES AND TRANSFER FUNCTIONS Continued

(a)  $M = 1.5$  ( $m = 1.86207$ )(c)  $M = 2.0$  ( $m = 2.00000$ )

$\theta$ , deg	$\theta'$ , deg	$\theta''$ , deg	S	H	T	$\delta$ , deg	$\delta_L$ , deg	$\theta$ , deg	$\theta'$ , deg	$\theta''$ , deg	S	H	T	$\delta$ , deg	$\delta_L$ , deg
0	0	0	1.003	+1.6667	-0.1071	0	180.00	0	0	0	1.625	+1.6667	0.2268	0	180.00
5	9.25	-8.95	1.466	+1.6346	-0.1068	3.43	167.04	5	13.13	-6.65	1.631	+1.6664	0.2258	6.76	168.99
10	18.18	-17.61	1.476	+1.5441	-0.1060	6.48	153.24	10	25.18	-13.23	1.649	+1.4571	0.2225	12.45	157.21
15	26.52	-25.75	1.494	+1.4085	-0.1047	8.79	137.43	15	35.55	-19.66	1.683	+1.2507	0.2166	16.63	143.52
20	34.13	-33.23	1.527	+1.2464	-0.1030	10.01	117.24	20	44.14	-25.89	1.744	+1.0266	0.2172	17.43	125.71
25	40.97	-40.01	1.594	+1.0850	-0.1019	9.34	85.17	25	51.19	-31.87	1.879	+0.8205	0.2066	15.80	93.97
30	47.19	-46.52	1.649	+1.0396	-0.1030	7.60	61.42	30	52.44	-33.04	1.939	+0.7633	0.1975	14.68	82.19
35	52.71	-51.74	1.693	+1.0249	-0.1050	5.38	40.20	35	53.65	-34.19	2.042	+0.7873	0.2029	12.45	63.44
40	57.50	-56.53	1.710	+1.0240	-0.1058	4.10	29.96	40	54.29	-34.76	2.134	+0.8051	0.2113	9.87	46.63
45	61.59	-60.61	1.733	+1.0254	-0.1071	0	0	45	54.74	-35.26	2.274	+0.8303	0.2258	0	0
50	65.02	-64.08	1.680	+0.8849	-0.0925	27.960	54.76	50	54.76	-35.26	2.179	+0.7905	0.2170	18.70	18.70
55	67.83	-66.89	1.674	+0.7831	-0.0820	27.968	54.79	55	55.44	-36.16	2.137	+0.6332	0.2161	16.61	16.61
60	70.00	-69.00	1.668	+0.7634	-0.0800	28.008	54.85	60	56.07	-36.84	2.000	+0.5014	0.2143	15.03	15.03
65	71.50	-70.50	1.662	+0.6973	-0.0733	28.138	54.96	65	56.99	-37.99	2.033	+0.4745	0.2175	12.75	12.75
70	72.38	-71.62	1.656	+0.6382	-0.0671	28.238	55.07	70	57.51	-38.51	1.932	+0.4146	0.2119	11.19	11.19
75	72.61	-71.81	1.653	+0.5913	-0.0624	28.338	55.19	75	57.19	-38.24	1.960	+0.3692	0.2100	10.00	10.00
80	72.29	-71.51	1.651	+0.5520	-0.0592	28.5	55.37	80	57.47	-38.47	1.920	+0.3123	0.2051	9.85	9.85
85	71.44	-70.66	1.650	+0.5296	-0.0564	29	55.92	85	57.92	-38.92	1.834	+0.2613	0.2013	9.59	9.59
90	70.00	-69.00	1.650	+0.5100	-0.0540	30	57.00	90	57.00	-39.65	1.731	+0.2852	0.2047	9.85	9.85
95	68.03	-67.03	1.650	+0.4900	-0.0520	32	59.03	95	59.03	-41.00	1.606	+0.1900	0.2059	10.00	10.00
100	65.43	-64.57	1.651	+0.4714	-0.0509	35	61.83	100	61.83	-42.97	1.487	+0.0795	0.2080	10.80	10.80
105	62.21	-61.79	1.653	+0.4542	-0.0504	40	65.92	105	65.92	-45.95	1.355	+0.1047	0.2136	11.36	11.36
110	58.44	-57.56	1.656	+0.4385	-0.0509	45	69.44	110	69.44	-49.99	1.262	+0.0696	0.2195	11.95	11.95
115	54.14	-53.86	1.660	+0.4242	-0.0527	50	72.53	115	72.53	-54.21	1.192	+0.0514	0.2260	12.60	12.60
120	49.40	-49.60	1.665	+0.4110	-0.0553	55	75.26	120	75.26	-58.19	1.138	+0.0380	0.2336	13.36	13.36
125	44.21	-44.79	1.670	+0.4000	-0.0585	60	77.78	125	77.78	-61.78	1.096	+0.0313	0.2420	14.20	14.20
130	38.56	-39.44	1.675	+0.3900	-0.0623	65	80.08	130	80.08	-65.02	1.064	+0.0262	0.2517	15.17	15.17
135	32.44	-33.56	1.680	+0.3810	-0.0665	70	82.23	135	82.23	-68.08	1.040	+0.0221	0.2620	16.20	16.20
140	25.85	-26.15	1.685	+0.3730	-0.0713	75	84.26	140	84.26	-71.29	1.022	+0.0193	0.2733	17.33	17.33
145	18.88	-19.12	1.690	+0.3660	-0.0765	80	86.22	145	86.22	-74.66	1.010	+0.0179	0.2853	18.53	18.53
150	11.53	-11.47	1.695	+0.3600	-0.0821	85	88.12	150	88.12	-78.16	1.002	+0.0175	0.2980	19.80	19.80
155	4.79	-4.71	1.700	+0.3550	-0.0880	90	90	155	90	-81.84	1.000	+0.0175	0.3113	21.13	21.13
160	0	0	1.705	+0.3510	-0.0940	95	91.83	160	91.83	-85.57	1.000	+0.0175	0.3253	22.53	22.53
165	0	0	1.710	+0.3480	-0.1000	100	92.83	165	92.83	-89.34	1.000	+0.0175	0.3400	24.00	24.00
170	0	0	1.715	+0.3460	-0.1060	105	93.83	170	93.83	-93.14	1.000	+0.0175	0.3553	25.53	25.53
175	0	0	1.720	+0.3450	-0.1120	110	94.83	175	94.83	-96.97	1.000	+0.0175	0.3713	27.13	27.13
180	0	0	1.725	+0.3450	-0.1180	115	95.83	180	95.83	-100.84	1.000	+0.0175	0.3880	28.80	28.80

(g)  $M = 2.5$  ( $m = 3.33333$ )(h)  $M = 3.0$  ( $m = 4.85714$ )

ch) $M = 3.0 \text{ } m = 3.85714$															
$\theta$ , deg	$\theta'$ , deg	$\theta''$ , deg	S	H	T	$\delta$ , deg	$\delta_L$ , deg	$\theta$ , deg	$\theta'$ , deg	$\theta''$ , deg	S	H	T	$\delta$ , deg	$\delta_L$ , deg
0	0	0	1.700	+1.6667	-0.3139	0	180.00	0	0	0	1.741	+1.6667	0.3754	0	180.00
5	16.26	-5.95	1.708	+1.5839	-0.3119	9.39	169.66	5	18.65	-5.62	1.751	+1.5610	0.3725	11.37	169.97
10	30.44	-11.86	1.734	+1.3774	-0.3055	16.57	158.51	10	34.22	-11.22	1.784	+1.3125	0.3631	19.48	159.10
15	41.77	-17.69	1.783	+1.1220	-0.2933	20.54	145.33	15	45.94	-16.78	1.845	+1.0270	0.3441	23.25	146.05
20	50.50	-23.43	1.869	+0.8638	-0.2722	21.12	127.29	20	54.54	-22.27	1.953	+0.7497	0.3068	22.74	127.56
20.832	51.75	-24.37	1.890	+0.8219	-0.2675	20.86	123.33	21	58.58	-25.52	2.072	+0.5894	0.2767	20.03	108.50
21.064	52.94	-25.31	1.913	+0.7807	-0.2625	20.50	118.87	25	59.79	-26.60	2.144	+0.5423	0.2658	18.56	97.65
22.496	54.08	-26.24	1.941	+0.7404	-0.2573	20.00	113.76	30	60.93	-27.68	2.307	+0.5271	0.2606	16.46	77.55
23.328	55.18	-27.18	1.976	+0.7014	-0.2519	19.36	107.69	35	61.26	-28.00	2.437	+0.5440	0.2871	15.13	64.65
24.160	56.23	-28.10	2.021	+0.6657	-0.2472	18.53	100.16	40	61.63	-28.37	2.940	+0.7137	0.3754	0	0
24.992	57.24	-29.03	2.086	+0.6325	-0.2448	17.42	89.96	45	61.63	-28.37	2.940	+0.7137	0.3754	0	0
25.824	58.24	-29.95	2.209	+0.6324	-0.2511	15.60	73.46	50	61.63	-28.37	2.940	+0.7137	0.3754	0	0
26.656	59.14	-30.86	2.496	+0.6324	-0.3139	0	0	55	61.63	-28.37	2.940	+0.7137	0.3754	0	0
26.675	59.16	-28.86	2.496	+0.6324	-0.2448	0	0	60	61.63	-28.37	2.940	+0.7137	0.3754	0	0
26.706	59.19	-27.57	2.413	+0.5129	-0.2108	0	0	65	61.63	-28.37	2.940	+0.7137	0.3754	0	0
26.736	59.25	-26.18	2.337	+0.3965	-0.1801	0	0	70	61.63	-28.37	2.940	+0.7137	0.3754	0	0
26.866	59.36	-24.16	2.244	+0.3470	-0.1437	0	0	75	61.63	-28.37	2.940	+0.7137	0.3754	0	0
26.956	59.46	-22.61	2.184	+0.2808	-0.1206	0	0	80	61.63	-28.37	2.940	+0.7137	0.3754	0	0
27.056	59.57	-21.25	2.138	+0.2469	-0.1032	0	0	85	61.63	-28.37	2.940	+0.7137	0.3754	0	0
27.492	60.04	-16.76	2.008	+0.1337	-0.0568	0	0	90	61.63	-28.37	2.940	+0.7137	0.3754	0	0
27.792	60.35	-14.29	1.949	+0.0966	-0.0373	0	0	95	61.63	-28.37	2.940	+0.7137	0.3754	0	0
28.328	60.90	-10.52	1.870	+0.0290	-0.0128	0	0	100	61.63	-28.37	2.940	+0.7137	0.3754	0	0
28.528	61.11	-9.26	1.846	+0.0129	-0.0057	0	0	105	61.63	-28.37	2.940	+0.7137	0.3754	0	0
28.750	61.33	-7.94	1.822	+0.0026	-0.0012	0	0	110	61.63	-28.37	2.940	+0.7137	0.3754	0	0
29.164	61.74	-5.63	1.781	+0.0266	-0.0121	0	0	115	61.63	-28.37	2.940	+0.7137	0.3754	0	0
29.264	61.84	-5.10	1.772	+0.0316	-0.0141	0	0	120	61.63	-28.37	2.940	+0.7137	0.3754	0	0
30	62.54	-1.46	1.715	+0.0614	-0.0290	0	0	125	61.63	-28.37	2.940	+0.7137	0.3754	0	0
35	66.81	16.66	1.476	+0.1288	-0.0752	0	0	130	61.63	-28.37	2.940	+0.7137	0.3754	0	0
40	70.33	29.31	1.340	+0.1276	-0.0632	0	0	135	61.63	-28.37	2.940	+0.7137	0.3754	0	0
45	73.30	39.24	1.246	+0.1109	-0.0528	0	0	140	61.63	-28.37	2.940	+0.7137	0.3754	0	0
50	75.87	47.46	1.177	+0.0906	-0.0487	0	0	145	61.63	-28.37	2.940	+0.7137	0.3754	0	0
55	78.14	54.51	1.126	+0.0705	-0.0426	0	0	150	61.63	-28.37	2.940	+0.7137	0.3754	0	0
60	80.17	60.74	1.087	+0.0522	-0.0353	0	0	155	61.63	-28.37	2.940	+0.7137	0.3754	0	0
65	82.04	66.37	1.057	+0.0364	-0.0272	0	0	160	61.63	-28.37	2.940	+0.7137	0.3754	0	0
70	83.77	71.55	1.035	+0.0234	-0.0186	0	0	165	61.63	-28.37	2.940	+0.7137	0.3754	0	0
75	85.40	76.42	1.019	+0.0132	-0.0105	0	0	170	61.63	-28.37	2.940	+0.7137	0.3754	0	0
80	86.97	81.06	1.008	+0.0059	-0.0059	0	0	175	61.63	-28.37	2.940	+0.7137	0.3754	0	0
85	88.50	85.57	1.002	+0.0015	-0.0015	0	0	180	61.63	-28.37	2.940	+0.7137	0.3754	0	0
90	90	90				0	0	185	61.63	-28.37	2.940	+0.7137	0.3754	0	0

TABLE I. WAVE ANGLES AND TRANSFER FUNCTIONS. Continued

(i) $M = 4.0$ ( $m = 4.57143$ )									(ii) $M = 6.0$ ( $m = 5.26829$ )								
$\theta$ , deg	$\theta'$ , deg	$\theta''$ , deg	S	R	T	$\delta_s$ , deg	$\delta_r$ , deg		$\theta$ , deg	$\theta'$ , deg	$\theta''$ , deg	S	R	T	$\delta_s$ , deg	$\delta_r$ , deg	
0	0	0	1.781	0.6667	-0.4515	0	180.00		0	0	0	1.816	0.6667	-0.3886	0	180.00	
5	21.80	-5.33	1.795	0.5269	-0.4471	13.95	170.26		5	21.75	-5.14	1.827	0.4966	-0.426	10.32	175.34	
10	38.87	-10.65	1.837	0.2248	-0.4327	22.80	150.60		10	32.89	-10.28	1.879	0.1422	-0.426	21.95	159.90	
15	50.77	-15.95	1.917	0.0087	-0.4029	25.94	146.55		15	51.69	-15.41	1.989	0.0009	-0.399	27.61	146.71	
20	58.90	-21.22	2.059	-0.6107	-0.3418	23.36	127.01		20	62.46	-20.52	2.162	-0.4878	-0.3194	22.32	125.78	
21.091	60.44	-22.36	2.106	-0.5444	-0.3204	21.88	120.57		21	63.69	-21.55	2.216	-0.4164	-0.3181	19.76	118.95	
22.182	61.79	-23.50	2.164	-0.4761	-0.2945	19.95	112.15		22	64.84	-22.57	2.282	-0.3360	-0.2972	16.75	109.37	
23.273	63.04	-24.64	2.251	-0.4090	-0.2669	17.48	99.12		23	65.91	-23.59	2.412	-0.2596	-0.2145	12.87	88.38	
23.5	63.29	-24.88	2.280	-0.3978	-0.2614	16.91	95.02		23.217 ( $\theta_r$ )	66.16	-23.84	3.004	-0.205	-0.1969	0	0	
24.0	63.83	-25.40	2.411	-0.3972	-0.2670	15.77	80.18		23.250	66.16	-22.95	3.192	-0.073	-0.117	0	0	
24.364 ( $\theta_r$ )	64.22	-25.78	3.288	-0.6000	-0.4515	0	0		24.297	66.21	-20.11	2.646	-0.002	-0.046	0	0	
24.370	64.22	-24.47	2.986	-0.4797	-0.3281				24.347	66.26	-18.62	2.511	0.066	0.015			
24.400	64.26	-22.77	2.743	-0.3604	-0.2303				24.417	66.36	-16.39	2.373	0.342	0.289			
24.464	64.32	-20.70	2.533	-0.2560	-0.1545				24.547	66.46	-14.66	2.291	0.616	0.613			
24.500	64.36	-19.84	2.492	-0.1900	-0.1006				24.647	66.56	-13.21	2.232	0.926	0.929			
24.564	64.42	-18.55	2.413	-0.1451	-0.1001				24	66.91	-9.41	2.095	0.796	0.693			
24.664	64.53	-16.87	2.327	-0.0976	-0.076				25	67.83	-6.03	1.896	1.125	1.298			
24.750	64.62	-15.65	2.273	-0.0885	-0.0476				27	69.57	-9.83	1.600	1.801	1.804			
24.764	64.63	-15.45	2.264	-0.041	-0.0446				30	71.80	-21.20	1.514	1.861	1.861			
25.000	64.87	-12.67	2.161	-0.0111	-0.0078				35	74.83	-31.49	1.340	1.650	2.396			
25.250	65.12	-10.20	2.084	-0.0256	-0.0182				40	77.25	-44.17	1.233	1.370	2.523			
25.773	65.63	-5.95	1.971	-0.0739	-0.0539				45	79.25	-51.77	1.161	1.100	2.96			
27.182	66.93	2.64	1.790	-0.1336	-0.1038				50	80.95	-58.05	1.111	0.876	2.644			
28.591	68.13	9.22	1.676	-0.1573	-0.1303				55	82.43	-63.40	1.075	0.650	2.677			
30	69.25	14.70	1.591	-0.1670	-0.1474				60	83.75	-68.11	1.050	0.473	2.500			
35	72.65	29.37	1.394	-0.1616	-0.1792				65	84.94	-72.34	1.032	0.371	2.716			
40	75.30	39.94	1.274	-0.1384	-0.1940				70	86.05	-76.23	1.019	0.297	2.728			
45	77.66	48.24	1.192	-0.1129	-0.2025				75	87.09	-79.87	1.010	0.116	2.737			
50	79.60	55.07	1.135	-0.0890	-0.2078				80	88.08	-83.34	1.004	0.051	2.742			
55	81.29	60.92	1.093	-0.0678	-0.2115				85	89.05	-86.70	1.001	0.013	2.745			
60	82.80	66.06	1.063	-0.0495	-0.2140				90	90	90						
65	84.18	70.68	1.041	-0.0342	-0.2158												
70	85.45	74.94	1.024	-0.0218	-0.2171												
75	86.65	78.92	1.013	-0.0122	-0.2180												
80	87.79	82.71	1.006	-0.0054	-0.2186												
85	88.90	86.38	1.002	-0.0013	-0.2189												
90	90	90															

(ki)  $M = 6.0$  ( $m = 6.000000$ )

$\theta$ , deg	$\theta'$ , deg	$\theta''$ , deg	S	R	T	$\delta_s$ , deg	$\delta_r$ , deg
0	0	0	1.833	0.6667	0.5832	0	180.00
5	27.70	-5.00	1.853	0.4503	0.5754	18.67	170.58
10	46.61	-10.00	1.918	0.0002	0.5484	28.05	160.10
15	58.12	-15.00	2.045	-0.7105	0.4873	28.51	146.67
20	65.40	-20.00	2.280	-0.3637	0.3253	19.33	123.90
20.552	66.03	-21.55	2.317	-0.3140	0.2889	17.12	119.67
21.104	66.64	-21.10	2.357	-0.2557	0.2421	14.29	114.51
21.656	67.23	-21.66	2.401	-0.1810	0.1761	10.35	107.57
22.208 ( $\theta_r$ )	67.79	-22.21	2.449	0.0000	0.0000	0	0
23.182	68.73	-4.93	1.971	-0.1586	0.665		
24.156	69.61	2.45	1.822	-0.1875	0.264		
25.130	70.44	8.09	1.721	-0.1963	0.2301		
26.104	71.21	12.78	1.643	-0.2036	0.2164		
27.078	71.94	16.85	1.579	-0.2039	0.2086		
28.052	72.63	20.47	1.525	-0.2018	0.2080		
29.026	73.28	23.72	1.479	-0.1981	0.2056		
30	73.90	26.69	1.438	-0.1935	0.2019		
35	76.61	38.83	1.287	-0.1638	0.2021		
40	78.77	47.71	1.192	-0.1334	0.2127		
45	80.54	54.76	1.130	-0.1060	0.2160		
50	82.04	60.54	1.087	-0.0822	0.2232		
55	83.34	65.48	1.058	-0.0619	0.2260		
60	84.50	69.82	1.037	-0.0449	0.2281		
65	85.56	73.73	1.023	-0.0308	0.2295		
70	86.53	77.31	1.013	-0.0196	0.2306		
75	87.44	80.66	1.007	-0.0109	0.2313		
80	88.32	83.86	1.003	-0.0048	0.2318		
85	89.16	86.96	1.001	-0.0012	0.2320		
90	90	90					

\* These values apply for  $\epsilon = 0$  only. For  $\epsilon = \infty$ , values should be replaced by 0. All other values are independent of  $\epsilon$ .

NACA Rept. 1233  
National Advisory Committee for Aeronautics.  
SHOCK-TURBULENCE INTERACTION AND THE  
GENERATION OF NOISE. H. S. Ribner. 1955.  
iii, 19p. diagrs., tab. (NACA Rept. 1233. Super-  
sedes TN 3255)

Interaction of convected field of turbulence with  
shock wave is analyzed to yield modified turbulence,  
entropy spottness, and noise generated downstream  
of the shock. Analysis is generalization of single-  
spectrum-wave treatment of TN 2864. Formulas  
for spectra and correlations are obtained. Numer-  
ical calculations yield curves of rms velocity com-  
ponents, temperature, pressure, and noise in db  
against Mach number for  $M = 1$  to  $\infty$ ; both isotropic  
and strongly axisymmetric (lateral/longitudinal  
= 36/1) initial turbulence are treated. In either  
case, turbulence of 0.1 percent longitudinal compo-  
nent generates about 120 dba of noise.

Copies obtainable from NACA, Washington

1. Flow, Supersonic (1.1.2.3)
2. Flow, Turbulent (1.1.3.2)
3. Noise (7.4)
- I. Ribner, Herbert  
Spencer
- II. NACA Rept. 1233
- III. NACA TN 3255



NACA Rept. 1233  
National Advisory Committee for Aeronautics.  
SHOCK-TURBULENCE INTERACTION AND THE  
GENERATION OF NOISE. H. S. Ribner. 1955.  
iii, 19p. diagrs., tab. (NACA Rept. 1233. Super-  
sedes TN 3255)

Interaction of convected field of turbulence with  
shock wave is analyzed to yield modified turbulence,  
entropy spottness, and noise generated downstream  
of the shock. Analysis is generalization of single-  
spectrum-wave treatment of TN 2864. Formulas  
for spectra and correlations are obtained. Numer-  
ical calculations yield curves of rms velocity com-  
ponents, temperature, pressure, and noise in db  
against Mach number for  $M = 1$  to  $\infty$ ; both isotropic  
and strongly axisymmetric (lateral/longitudinal  
= 36/1) initial turbulence are treated. In either  
case, turbulence of 0.1 percent longitudinal compo-  
nent generates about 120 dba of noise.

Copies obtainable from NACA, Washington

NACA Rept. 1233  
National Advisory Committee for Aeronautics.  
SHOCK-TURBULENCE INTERACTION AND THE  
GENERATION OF NOISE. H. S. Ribner. 1955.  
iii, 19p. diagrs., tab. (NACA Rept. 1233. Super-  
sedes TN 3255)

Interaction of convected field of turbulence with  
shock wave is analyzed to yield modified turbulence,  
entropy spottness, and noise generated downstream  
of the shock. Analysis is generalization of single-  
spectrum-wave treatment of TN 2864. Formulas  
for spectra and correlations are obtained. Numer-  
ical calculations yield curves of rms velocity com-  
ponents, temperature, pressure, and noise in db  
against Mach number for  $M = 1$  to  $\infty$ ; both isotropic  
and strongly axisymmetric (lateral/longitudinal  
= 36/1) initial turbulence are treated. In either  
case, turbulence of 0.1 percent longitudinal compo-  
nent generates about 120 dba of noise.

Copies obtainable from NACA, Washington

1. Flow, Supersonic (1.1.2.3)
2. Flow, Turbulent (1.1.3.2)
3. Noise (7.4)
- I. Ribner, Herbert  
Spencer
- II. NACA Rept. 1233
- III. NACA TN 3255



NACA Rept. 1233  
National Advisory Committee for Aeronautics.  
SHOCK-TURBULENCE INTERACTION AND THE  
GENERATION OF NOISE. H. S. Ribner. 1955.  
iii, 19p. diagrs., tab. (NACA Rept. 1233. Super-  
sedes TN 3255)

Interaction of convected field of turbulence with  
shock wave is analyzed to yield modified turbulence,  
entropy spottness, and noise generated downstream  
of the shock. Analysis is generalization of single-  
spectrum-wave treatment of TN 2864. Formulas  
for spectra and correlations are obtained. Numer-  
ical calculations yield curves of rms velocity com-  
ponents, temperature, pressure, and noise in db  
against Mach number for  $M = 1$  to  $\infty$ ; both isotropic  
and strongly axisymmetric (lateral/longitudinal  
= 36/1) initial turbulence are treated. In either  
case, turbulence of 0.1 percent longitudinal compo-  
nent generates about 120 dba of noise.

Copies obtainable from NACA, Washington

1. Flow, Supersonic (1.1.2.3)
2. Flow, Turbulent (1.1.3.2)
3. Noise (7.4)
- I. Ribner, Herbert  
Spencer
- II. NACA Rept. 1233
- III. NACA TN 3255

